BRNO UNIVERSITY OF TECHNOLOGY

VYSOKÉ UČENÍ TECHNICKÉ V BRNĚ

FACULTY OF ELECTRICAL ENGINEERING AND COMMUNICATION

FAKULTA ELEKTROTECHNIKY
A KOMUNIKAČNÍCH TECHNOLOGIÍ

DEPARTMENT OF BIOMEDICAL ENGINEERING

ÚSTAV BIOMEDICÍNSKÉHO INŽENÝRSTVÍ

DETECTION OF HIGH-FREQUENCY EEG ACTIVITY IN EPILEPTIC PATIENTS

DETEKCE VYSOKOFREKVENČNÍ EEG AKTIVITY U EPILEPTICKÝCH PACIENTŮ

DOCTORAL THESIS
DIZERTAČNÍ PRÁCE

AUTHOR — **Ing. Mgr. Jan Cimbálník**
AUTOR PRÁCE

SUPERVISOR — **Ing. Pavel Jurák, CSc.**
ŠKOLITEL

BRNO 2016

ABSTRAKT

Tato práce se zabývá automatickou detekcí vysokofrekvenčních oscilací jakožto moderního elektrofyziologického biomarkru epileptogenní tkáně v intrakraniálním EEG, jehož vizuální detekce je zdlouhavý proces, který je ovlivněn subjektivitou hodnotitele. Epilepsie je jedním z nejčastějších neurologických onemocnění postihující 1 % obyvatelstva. Přestože jsou přibližně dvě třetiny případů léčitelné farmakologicky, zbylá třetina pacientů je odkázána zejména na léčbu chirurgickým zákrokem, pro nějž je zapotřebí přesně lokalizovat ložisko patologické tkáně. Vysokofrekvenční oscilace jsou v posledním desetiletí studovány pro jejich potenciál lokalizace patologické tkáně. Součástí této práce je shrnutí dosavadního výzkumu vysokofrekvenčních oscilací a výčet detektorů používaných ve výzkumu. V rámci práce byly vyvinuty či vylepšeny tři detektory vysokofrekvenčních oscilací, na jejichž popis navazuje evaluace z hlediska shody s manuální detekcí, přesnosti výpočtu příznaků oscilací a schopnosti lokalizace patologické tkáně. V závěru práce jsou představeny vyvinuté metody vizualizace vysokofrekvenčních výskytu oscilací a stručně uvedeny dosažené vědecké výsledky.

KLÍČOVÁ SLOVA

Epilepsie, zóna počátku záchvatu, vysokofrekvenční oscilace, detekce vysokofrekvenčních oscilací.

ABSTRACT

This work deals with automated detection of high-frequency oscillations as a novel electrophysiologic biomarker of epileptogenic tissue in intracranial EEG. Visual detection of these oscillations is a time-consuming process and is prone to reviewer bias. Epilepsy is one of the most common neurological diseases affecting 1 % of population. Even though two thirds of cases are successfully treated with anti-epileptic drugs, the rest of the patients are dependent mainly on surgical procedure, which requires precise localization of pathologic focus. High-frequency oscillations have been studied over the last decade for their potential to localize the focus of pathological tissue. Initial part of this work is a summary of the current state of high-frequency oscillations research and a detailed list of detectors used in research. Within the scope of this work three high-frequency oscillation detectors were developed or enhanced. The description of the algorithms is followed by detector evaluation with regard to the concordance with expert reviewed events, feature estimation and the ability to correctly localize pathological tissue. The final part of the work provides an overview of developed visualization methods and a short summary of achieved scientific results.

KEYWORDS

Epilepsy, seizure onset zone, high-frequency oscillations, detection of high frequency oscillations.

CIMBÁLNÍK, J. *Detekce vysokofrekvenční EEG aktivity u epileptických pacientů.* Brno: Vysoké učení technické v Brně, Fakulta elektrotechniky a komunikačních technologií, 2016. 85 s., 4 s. příloh. Vedoucí práce Ing. Pavel Jurák, CSc.

PROHLÁŠENÍ

Prohlašuji, že svou dizertační práci na téma Detekce vysokofrekvenční aktivity u epileptických pacientů jsem vypracoval samostatně pod vedením vedoucího disertační práce a s použitím odborné literatury a dalších informačních zdrojů, které jsou všechny citovány v práci a uvedeny v seznamu literatury na konci práce.

Jako autor uvedené práce dále prohlašuji, že v souvislosti s vytvořením této práce jsem neporušil autorská práva třetích osob, zejména jsem nezasáhl nedovoleným způsobem do cizích autorských práv osobnostních a/nebo majetkových a jsem si plně vědom následků porušení ustanovení § 11 a následujících zákona č. 121/2000 Sb., o právu autorském, o právech souvisejících s právem autorským a o změně některých zákonů (autorský zákon), ve znění pozdějších předpisů, včetně možných trestněprávních důsledků vyplývajících z ustanovení části druhé, hlavy VI. díl 4 Trestního zákoníku č. 40/2009 Sb.

V Brně dne ....

(podpis autora)

PODĚKOVÁNÍ

Děkuji vedoucímu své dizertační práce Ing. Pavlu Jurákovi, CSc. za účinnou metodickou, pedagogickou a odbornou pomoc a další cenné rady při zpracování mé disertační práce. Dále děkuji Prof. Milanu Brázdilovi a kolegům v laboratoři Mayo Systems Electrophysiology Lab, Mayo Clinic za předání cenných vědomostí v průběhu zpracování mé práce. V neposlední řadě děkuji své manželce a rodině za všeobecnou podporu.

V Brně dne ....

(podpis autora)

CONTENT

LIST OF FIGURES

LIST OF TABLES

LIST OF EQUATIONS

INTRODUCTION

Epilepsy is a group of diseases which affect the brain of the patients and significantly impairs their quality of life and limits them in their everyday activities. About 60 % of epileptic patients can be treated with antiepileptic drugs, however, the remaining 30 % of patients have to undergo a surgery to remove epileptogenic tissue causing their seizures. Even though the surgery is a highly invasive procedure the positive outcome is never guaranteed due to poor localization of pathological part of the brain.

Nowadays the localization of the epileptogenic focus is done by a number of methods, including scalp electroencephalography, magnetic resonance imaging and neuropsychologic examination. If the results of these examinations are inconclusive, the patient undergoes an electrode implantation to map the seizure onset zone in the brain. While seizure onset zone is located in majority of the cases, the resection of the tissue often does not bring seizure freedom to the patients. Thus, other biological markers of epileptogenic tissue, which would correctly localize the pathologic tissue, are essential for good outcome of the surgery.

High frequency oscillations (HFOs) in frequencies ranging from 80 - 600 Hz are a relatively novel and promising electrophysiological biomarker that could improve localization of epileptogenic focus and help the physicians minimize the resection area while achieving better surgery outcome and protecting the functional brain sites necessary for everyday life of the patient. Apart from being linked to the epileptogenic foci, they are also present in healthy brain during cognitive processing. Distinguishing between the physiological HFOs and pathological ones is one of current endeavors of neuroscientists.

Manual revision and marking of high frequency oscillations is a time consuming process and is prone to reviewer bias. Moreover, interviewer concordance is often poor leading to discrepancies in the analyses. Therefore, an objective, robust and fast method is needed to eliminate the drawbacks of visual detection. Development of such algorithm is hindered by an unclear HFO definition.

To date a number of detectors based on different HFO features and signal metrics have been developed but most of them were applied on preselected data sets or animal recordings solely for research work. Moreover, evaluation of the detectors is not uniform which makes them nearly impossible to compare.

The aim of this work is to develop and evaluate high-frequency oscillation detectors that are robust and feasible for clinical application and research. Such tools could provide physicians with valuable information about the patient's brain and could improve the well being of patients while reducing the costs of their stay in hospital. It also allows for studying HFOs in cognition and broadening the knowledge of brain processing.

Three detectors were developed or improved within this work. One based on well known line-length metric, second which uses a novel frequency homogeny metric to overcome effects of Gibb's phenomenon and third based on normalized Hilbert transformed signals.

All detectors were evaluated from three different perspectives. Agreement between human scored events and automated detection was evaluated using precision-recall analysis. Correctness of feature estimation was assessed with the use of artificial events and comparison of their set features with automatically computed features. Lastly, the ability of the detectors to correctly localize pathological tissue was measured using pathological channels marked by expert reviewers and resected areas in patients with good surgical outcome.

To provide clinicians and researchers with information about HFO occurrence and their features three visualization methods developed for this purpose are presented. One is based on HFO rates in individual frequencies, other uses MRI scans to simultaneously provide information about the anatomy of the studied brain and the last one providing information about HFO rates, their features and brain connectivity.

The results of this work are currently being used in St. Anne's University Hospital in Brno, Czech Republic and Mayo Systems Electrophysiology Laboratory at Mayo Clinic, USA. Further work will focus on algorithm optimization, on-line implementation and HFO clustering.

1 EPILEPSY DIAGNOSTICS AND MARKERS

Epileptic seizures and epileptic syndromes have high prevalence and incidence rates affecting both sexes, all ages and all races. Their estimated incidence ranges between 0.5 % and 1 % [1]. They constitute an important part of everyday neurological practice and are listed among the most frequent neurological diseases along with Parkinson's and Alzheimer's disease.

Epilepsy is not a single disease entity but rather a group of many syndromes and diseases that have a multitude of various manifestations and causes. Therefore, the definition of epilepsy is not clear and there is no consensus. The newly proposed definition by International League Against Epilepsy is: "*Epilepsy is a disorder of the brain characterized by an enduring predisposition to generate epileptic seizures and by the microbiological, cognitive, psychological and social consequences of this condition*" [2]. This definition requires the occurrence of at least one epileptic seizure with the precondition that it is in association with an enduring disturbance of the brain capable of giving rise to other seizures. This proposal has been, however, criticized by lead epidemiologists.

1.1 Epilepsy throughout the history

Epilepsy has been known for at least 3000 years [3]. In the past epilepsy was considered to be something supernatural, daemonic or divine, due to inexplicable causes of the disease. Hence, the common people of the time gave the disease names like "Sacred disease" or "God's disease". The perception of epilepsy as a god's punishment led to similar irrational ideas about its treatment. Common middle-age treatment included herbal teas often prepared in special conditions and during special rites [4].

Even though epilepsy was considered sacred, some philosophers and doctors studied epilepsy and claimed that epilepsy has organic causes rather than divine. Among

them for example a Greek philosopher Hippocrates who stated that: ”*Epilepsy is a natural rather than divine disease. The seizures begin in the brain.*” or a Swiss German alchemist Paracelsus: ”*Epilepsy is an organic rather than mythic disease. Even animals can suffer from epilepsy. The causes of the disease are not always treatable but the symptoms are.*”[4]

The invention of electroencelphalography (EEG) by Hans Berger in 1924 led to better understanding of epilepsy and confirmed its localization in the brain. EEG is still the most used technique in diagnosis and management of epilepsies but fast emerging field of neuroimaging enables physicians to deeper understand the processes in the brain as well as the underlying pathologies of epilepsy.

1.2 Epilepsy treatment and pharmacoresistant epilepsies

The ultimate aim of epilepsy treatment is total seizure freedom with no clinically significant adverse effects. This is nowadays broadened to include optimal outcomes of health-related quality of life with regard to physical, mental, educational, social and psychological state of the patient. The majority of epilepsies are successfully treated with anti-epileptic drugs (AEDs) in continuous prophylactic schemes with drug mixtures tailored to each patient. However, AEDs are ineffective for about 20 % of epileptic patients. These patients are candidates for neurosurgical interventions, other pharmacological or non-pharmacological treatments.

The surgical treatment of drug-resistant epilepsy has become increasingly more valuable and often life-saving due to recent advances in structural and functional neuroimaging, EEG monitoring and sophisticated surgical techniques. The outcome of surgical methods has improved dramatically for both adults and pediatric patients. Early successful surgical intervention might prevent or even reverse the disabling psychological consequences of uncontrolled seizures during critical periods of personality development. Despite the advances and better outcomes, surgery in epilepsies is often not performed or delayed due to fear of patients or physicians about the surgery. The surgery is then often substituted with newer AEDs, vagus nerve stimulation or deep brain stimulation devices which, however, often fail to deliver appropriate medical treatment [5].

A successful surgical intervention requires the epileptogenic tissue to be well localized, and located in the brain area that can be removed safely without significantly impairing the normal function of the brain. The correct localization of the pathological tissue is often crucial for the surgery to have a good outcome by achieving seizure freedom for the patient. Despite the development of neuroimaging diagnostic methods, additional information is often needed to better localize the focus of epileptic seizures. This information is provided by the intracranial EEG (iEEG) which involves highly invasive, albeit necessary, craniotomy procedure or access to the brain through holes drilled in the skull and implantation of depth or/and subdural electrodes.

1.3 Epilepsy diagnostic tools and epilepsy markers

Medical technologies have an increasing impact on diagnosis and treatment in all areas of medicine. More so on epilepsy where the use of technologies is inevitable due to relative inaccessibility of the brain. Nowadays epileptologists have a wide array of methods to choose from but not all of them are suitable for epilepsy diagnostics. This section discusses the technologies used in clinical practice as well as in research.

1.3.1 Neuropsychological testing

Neurophysiological testing is nowadays an established method for examination of surgical candidates. The role of this examination is mainly to evaluate cognitive deficits related to epilepsy. However, a standard battery of tests is not defined. Such battery should cover at least one test targeting: episodic memory, executive function, language, visuoconstructional functions, psychomotor speed, speech, and attention [6].

1.3.2 EEG and video-EEG in epilepsy diagnosis

EEG methods are a well established tool in neurology and are commonly used for brain diagnostics.

The classical EEG, which is entirely harmless and relatively inexpensive, is the most important investigative tool used in diagnosis and management of epilepsies. The EEG is indispensable in the correct diagnosis of the type of epileptic seizure or the

syndrome these patients may have. Nowadays the EEG is an integral part of epilepsy diagnostic process and is mandatory for all patients with epileptic seizures.

Unlike conventional EEG, video-EEG is the means of reaching an incontrovertible diagnosis if clinical events occur during the recording. These may be incidental or predictable based on circadian cycle or triggering stimuli. Video-EEG machines are becoming affordable mainly due to advances in digital compression and storage technology. The main reason to use video-EEG is to capture minor symptoms which might have clinical value but are hard to notice by medical staff.

1.3.3 iEEG in pharmacoresistant epilepsies

Compared to the two above mentioned methods iEEG is highly invasive and expensive. For this reason it is solely used in patients with pharmacoresistant focal epilepsies as a method for precise localization of epileptogenic focus. The implantation of iEEG electrodes is preceded by classical EEG evaluation and neuroimaging techniques. When the rough focus localization is achieved the patient undergoes an implantation surgery. Once implanted the electrophysiological signals can be recorded directly from the brain tissue allowing for an in-depth evaluation of small areas of the brain and precise localization of seizure onset zone (SOZ).

The indubitable advantage of this approach is the direct contact with brain tissue and possibility to record signals which are impossible to be captured with conventional EEG or neuroimaging [7]. Apart from seizures themselves there are a few interictal biomarkers of epileptogenic tissue. Widely accepted biomarkers are epileptiform spikes and sharp waves. These interictal EEG signatures of epileptic brain are generated by the paroxymal discharge of large neuronal populations and are highly specific for epilepsy [8]. Apart from interictal epileptiform discharges (IEDs), recent studies suggest that HFOs are an interictal signature of epileptogenic networks. While IEDs are specific for epileptogenic brain, they are not an ideal biomarker because they are only loosely related to disease activity unless accompanied by other phenomena [9]. They are not a good indicator of seizure occurrence and do not fluctuate as seizures do in relation to AED treatment [10]. Since HFOs are the focus of this work their clinical value and characteristics are described separate chapter (3).

1.3.4 Neuroimaging in epilepsy diagnostics

Modern structural and functional brain imaging has had a huge impact on diagnosis and managements of epilepsies. The enormous amount of anatomical and metabolic data has led to greater insights into pathophysiology underlying symptomatic epilepsy and can contribute immensely to the elucidation of the various forms of epilepsies.

MRI

Magnetic resonance imaging (MRI) is the superior of all structural imaging tools in terms of epilepsy. MRI abnormalitites are present in 80 % of patients with refractory focal seizures and 20 % of the patients with single unprovoked seizures or epilepsy in remission [5]. MRI is greatly superior to computed tomography (CT) with regard to its sensitivity and specificity for identifying subtle abnormalities.

In case the lesion is found the patient has an increased chance of achieving seizure freedom after a correct resection [11]. To achieve a correct MRI evaluation, two main conditions have to be fulfilled. First, the MRI scan has to be evaluated by an experienced neurologist. It has been proved that the chance of discovering an abnormality on a standard MRI is 50 % when assessed by and expert compared to a non-expert neuro-radiologist whose chance is only 40 %. Second, the MRI protocol should be tailored to epilepsy. Using a tailored MRI measurement protocol the chance of expert neuro-radiologist discovering a lesion is substantially increased to 90 % [12]. Such protocol was proposed by Wellmer et al. [13].

Computed Tomography

CT can be used for detection of gross structural lesions but, as stated above, will miss small lesions, including tumors, vascular malformations, hippocampal sclerosis and most malformations of cortical development [5]. Nevertheless, CT may be occasionally useful when MRI is not readily available or cannot be performed for technical reasons (i.e. implanted cardiac pacemakers, cochlear implant or even iEEG electrodes).

Positron emission tomography

Positron emission tomography (PET) is an important functional imaging method for evaluation of SOZ localization. In common practice, interictal PET is done with a glucose analogue substance, namely fluorine-18fluorodeoxyglucose, used as a tracer. The tracer is an indirect marker of neuronal activity. In interictal PET images epileptogenic area appears as hypometabolic area. PET can be evaluated by simple visual analysis, however, the results are known to be associated with significant variability between investigators. To overcome this problem, two approaches have been developed. First, comparison of glucose metabolic rate in the region of interest to control group dataset. Second, voxel-based approach using statistical parametric mapping and asymmetry index [14, 15].

Single photon emission computed tomography and SISCOM

Single photon emission computed tomography (SPECT) with cerebral blood flow agents is useful for supporting the localization of focal epilepsy when it is performed in a carefully monitored ictal or early post-ictal examination compared with inter-ictal scan. This may be used as part of pre-surgical evaluation and help guide the placement of iEEG electrodes if other data, including structural imaging, are equivocal or not concordant. In apparently generalized epilepsies, ictal SPECT may be helpful to identify a focal component. In interictal periods the SOZ area show hypoperfusion of the tissue, contrary to hyperperfusion at the beginning of seizures and during seizures. A common technique, which utilizes this effect to improve the anatomical determination of the abnormalities in cerebral blood flow, is the co-registration of interictal with either ictal or post-ictal SPECT images with a patient's MRI which forms Substraction Ictal SPECT Coregistred to MRI image commonly referred to as SISCOM. An example of such image is in Figure 1. Even though is method showed good correspondence with SOZ, there are some factors limiting this method [16].

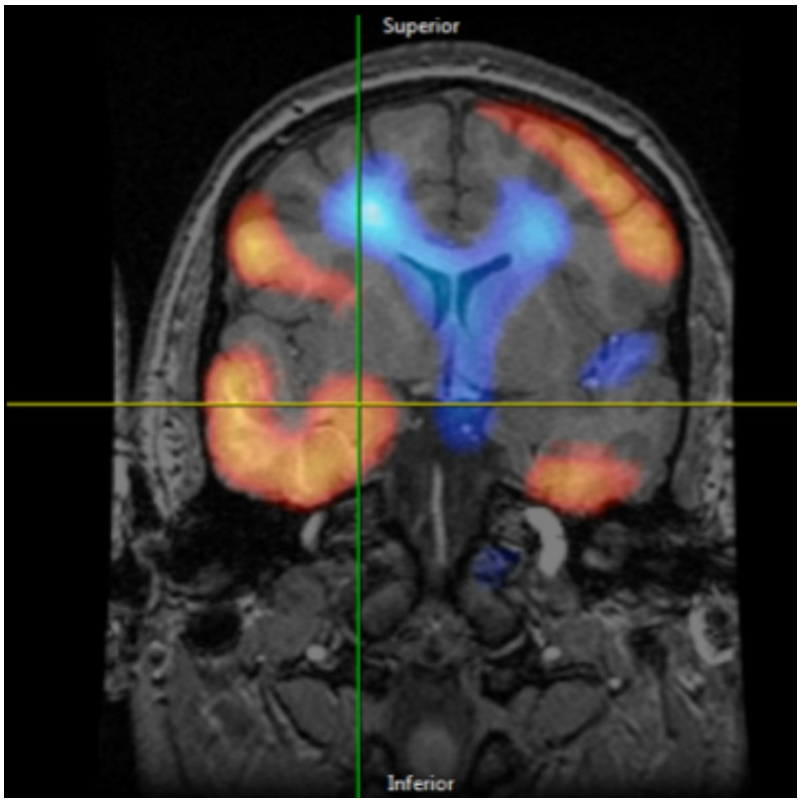

Figure 1: ***Ictal difference image of epileptic brain.***

The image shows ictal difference image with areas highlighting neuronal desynchronization (blue) and neuronal synchronization (orange). The cross is placed in the area of seizure onset zone.

Functional MRI and Magnetoencephalography

Functional MRI (fMRI) is not currently indicated for clinical reasons. However, this situation is changing and in many epilepsy centers fMRI of the blood oxygen level-dependent contrast is being used to localize the functional areas of the brain.

Magnetoencephalography (MEG) is a promising non-invasive and non-hazardous technology of functional brain mapping that is still in development. It is used to identify both normal and abnormal brain function. MEG records externally, from the scalp, the weak magnetic forces generated by neuronal electrical activity of the brain. It provides localized cortical areas with a great degree of accuracy, generating maps with high spatial and temporal resolution.

2 INTRACRANIAL EEG SIGNAL

Intracranial EEG signal differs form the classic scalp EEG in numerous ways. First of all, the size and shape of iEEG electrodes is adjusted to their application in the brain. Compared to scalp EEG, where summarized local field potentials are recorded, the smaller sized intracranial electrodes allow for recording brain activity directly at the source, which can be at the surface of the brain (subdural electrodes) or in the deeper structures of the brain (depth electrodes). Due to its highly invasive nature, the number and position of electrodes is determined solely by clinical needs which leads to only limited spatial sampling of the iEEG signal and could also lead to an imprecise placement of electrodes, thus missing the epileptogenic focus. Since the iEEG signal is recorded directly from the tissue, low amplitude high frequency signals can be acquired because they are not damped by the skull. That requires appropriate recording device with sufficient sampling frequency, quantization step and dynamic range. Intracranial EEG signals do not suffer from myopotential noise as much as scalp EEG, nonetheless, given their low amplitude they are more prone to environmental noise such as produced by leads in walls and surrounding devices. In this regard, the methodology, reference and the environment where the recording takes place, are essential for signal quality and subsequent processing.

2.1 Source of iEEG signal

Compared to conventional scalp EEG intracranial EEG signal is recorded from much smaller area and at the source of the signal. The signal recorded by clinical macro contacts consists mostly of local field potentials (LFPs) but can be influenced by far field potentials (FFPs) as well.

Despite extensive research the origin of local field potentials is still not well understood. However, recent findings suggest that the LFPs are mostly produced by synaptic currents and their return currents. Another factor contributing less to the final signal are spikes generated by neurons[17]. LFPs appear to be generated mainly by

synaptic inputs and associated return currents. The position of the electrode with regard to neuronal cells in crucial in this regard. Signal recorded near the soma of a neuron can have different shape, amplitude and polarity than the signal recorded from the dendrite tree of the neuron [17]. Although, LFPs signals are dominated by the synaptic activity, other phenomena such as spikes produced by sodium channels. The locality of the LFP, that is, the network activity generating the signal is still not fully understood. Studies carried out to shed light on this problem yielded conflicting results [17].

When analyzing both EEG and iEEG, brain tissue characteristics should be taken into account. A well documented volume conduction problem is caused by anisotropic characteristics of brain tissue, which has different conductivity in different areas of the brain and is also influenced by age, disease state and environmental factors. When localizing the source of the signal, volume conduction can significantly distort the results. More so in iEEG, where implantation of electrodes creates an abnormal environment for the brain [18]. Apart from the holes in the skull necessary for electrode implantation, the areas around electrodes show traces of microhemorrhages and the body reacts to an alien object in the body by scaring and inflammation [19]. This can further enhance the effect of volume conduction by creating a layer of liquid along the electrodes.

2.2 Intracranial electrode types

An important aspect with an impact on the acquired data is the electrode shape, size and implant location. Intracranial electrodes can be divided into two basic categories based on their implantation site:

- Subdural electrodes – have the shape of small disks that are placed under the dura mater onto the neocortex in form of arrays as grids or strips (Figure 2). The main drawback of this type of electrodes results from the method of implantation which requires craniotomy. The contact between the electrode and the tissue is often drying out which results in worse signal transmission and introduces noise into the recording even though the implantation area is kept moist by the medical staff. While craniotomy might seem as a highly invasive approach the implantation has lower risks than the use of depth electrodes.

- Depth electrodes – are commonly placed on a flexible plastic wire (Figure 3). They are inserted directly into the brain tissue, therefore avoiding the drying out drawback of the subdural electrodes. This results in better signal to noise ratio. Depth electrodes can be inserted into deep structures to record from a close proximity of the source. This leads to risk of blood vessel rupture during implantation, which is around 2 % [20].

Electrode types can be further divided into clinical macro-electrodes and research micro-electrodes. While the first type is used in clinic regularly the latter serves mainly for research purposes. The differences in signal stem from the size of the electrode as well as from the size of the tissue they record from. The macro electrodes have size of about 10 mm^2 and record from ~1000 neurons while micro electrodes record 100 – 10 neurons with the diameter of approximately 40 μm. Micro electrodes on subdural grids are in form of miniscule discs in spaces between clinical macro contacts. Micro contacts on depth electrodes can have two forms – shafts, which are embedded between the clinical macro electrodes in a circle around the needle, or bundles, which have a form of microwires at the tip of the depth electrode. Because of their small size micro electrodes can record single unit activity. The physical size of the micro electrodes is ~10 times smaller than of the macro electrodes which makes their implantation challenging as well as makes them prone to noise due to weak signals they record.

Even though intracranial electrodes present a unique opportunity to record electrical brain activity directly from the source, the spatial resolution of the acquired signal is unsatisfactory due to electrode placement, which is directed solely by clinical decision. The optimal electrode cross-section and spacing for mapping epileptic brain is still not known.

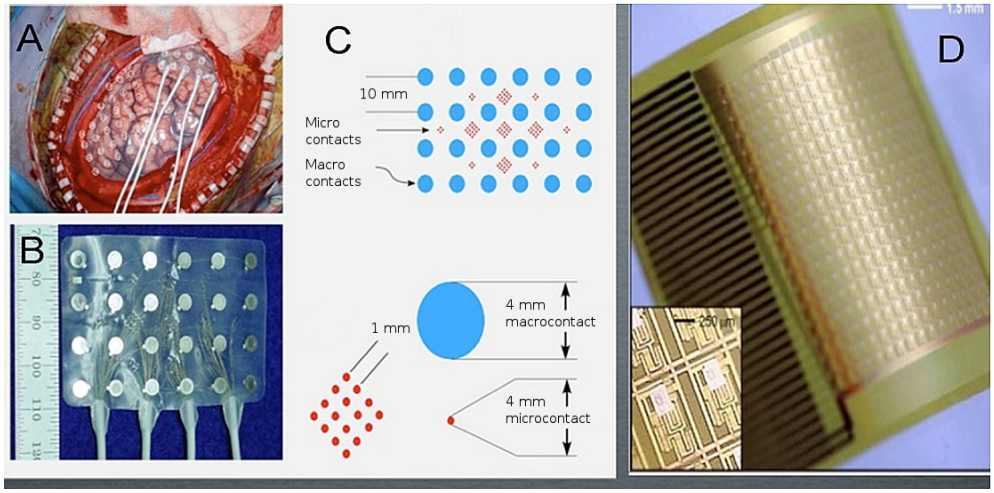

Figure 2: ***Types of subdural, non-penetrating electrodes.***

(A) Implant of hybrid subdural electrodes. (B) Hybrid subdural electrode grid composed of 24 clinical macroelectrodes. (C) Schematics of electrodes shown in (B) with macroelectrodes marked in blue and intercalated microelectrode arrays in red. (D) Flexible thin film electrodes with integrated electronics and 10µm electrode spacing.[7]

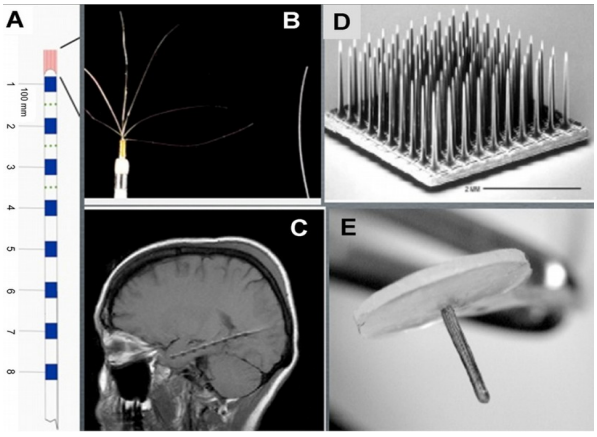

Figure 3: ***Penetrating depth electrodes.***

(A) Schematic of penetrating depth electrode with 8 macroelectrodes in blue and microelectrodes in red on the tip and embedded into the shaft between the macroelectrodes. (B) Enlarged depth-electrode tip showing 40 µm diametr wires exiting the tip. (C) MRI showing implanted depth electrode into temporal lobe structures. (D) Utah array composed of 100 microelectrodes that penetrate the cortex. (E) Thubtack microelectrode array that penetrates the cortex. The microelectrodes are in an array along the shaft.[7]

2.3 Intracranial EEG recording devices

Even though a standard EEG recording device can be used to acquire iEEG signals, it has a significant impact on the recorded data due to the high frequency and low amplitude nature of the data. The basic characteristics such as sampling frequency, bit depth and dynamical bandwidth play a crucial role in iEEG signal acquisition. Low sampling frequency restricts the frequency bandwidth for analysis, high bit depth is necessary to correctly record low amplitude events and dynamical bandwidth is necessary to avoid signal saturation.

Historically, sampling frequencies of iEEG acquisition systems were set to record well known Berger bands – delta (0.1 – 3 Hz), theta (4 – 7 Hz), alpha (8 – 15 Hz) and beta (16 – 31 Hz) rhythms. Recent studies, however, revealed that gamma frequencies (25 – 80 Hz) as well as high-frequency oscillations are involved in cognitive function and pathology [10]. This has led to increase of sampling frequencies in clinical acquisition systems up to 32 kHz to allow for analysis of high frequency components of iEEG signals.

Due to 1/f nature of EEG the bit depth of recording devices had to rise according to sampling frequency. High-frequency oscillations can exhibit amplitudes as low as 100 μV. In cutting edge devices the bit depth is 24 bits.

The quality of individual hardware components is essential since they can produce artifacts into the acquired data and therefore complicate the subsequent signal analysis. In case of HFOs this often leads to many false positive detections and could potentially cause an incorrect localization of pathological tissue.

One of the most common machine artifact results from lost bits during the recording. That creates a delta function in the data. Since frequency decomposition of a delta function contains all frequencies the artifact poses a problem when filtering the data because it creates higher amplitude of the filtered signal at the artifact position.

2.4 Methods of intracranial data acquisition

However, recorded signals are not subject only to technical differences. Data acquisition methods as well as the environment in which the signal is acquired play an important role. Some epilepsy centers record iEEG signals in clinical wards without giving any further instructions to the patient. Such signals are often degraded by ambient noise produced by other medical devices or by patient's movement. By instructing the patient to lay still and using shielded rooms can immensely improve the quality of the data which is the key to valid analysis.

Apart from the ambient in which the signals are acquired the brain state plays an important role. Implanted patients often undergo some kind of brain stimulation for basic research such as visual or motor tasks. Brain stimulation can influence the occurrence of biological markers. Another physiological state that is known to have an impact on electrophysiological markers is sleep. The depth of sleep changes power of frequencies in recorded signals and is closely linked to electrophysiological signals, especially HFOs [21].

While brain states define the temporal changes in the data, anatomical location of implanted electrodes defines the spatial differences and influences the data due to neuronal wiring of the brain and distinctive histological tissue. Archicortex and especially hippocampus are known to produce more HFOs and are more epileptogenic than neocortex [22].

2.5 Reference electrodes and montages

Reference for iEEG signal acquisition as well as used electrode can have a significant impact on the recorded data. Chosen recording reference and montage depends on the historical needs of the institution, available equipment and requirements on the recorded signal.

So called unipolar or referential montage can be applied in a few different ways by choosing the reference electrode. This type of montage is typically used for clinical recording. There is no universal reference and each approach has its advantages and

disadvantages. Virtual reference is used as the average signal of all recording channels. While this reference makes the individual lead signals more resistant to low-amplitude noise it can cause propagation of high-amplitude noise or pathological signal, such as seizure, from one lead to the rest of the leads making it somewhat more difficult to locate SOZ. Another approach, which is more traditional, is to use one reference electrode on the scalp or ear lobule. This reference method is prone to introducing outside noise, such as movement, from the reference lead.

A not so common approach is to choose a reference electrode or an average from number of contacts located in the area of the brain that is not very active, typically the white matter. Myopotentials and ambient noise are reduced by this configuration but some basal activity from the white matter is introduced into the recording. Moreover, this approach requires localization of contacts in MRI images by clinicians. Such configuration produces true unipolar intracranial EEG data that are suitable for research.

Biopolar montage utilizes two electrode contacts in the brain, which are usually spatially close to each other, by comparing their electrical potential. This approach creates a signal that is a product of local field potentials between those two electrodes. This montage is often used for studying a specific area of the brain such as motor cortex or limbic system during cognitive tasks.

3 HIGH-FREQUENCY OSCILLATIONS

High-frequency oscillations (HFOs) are electrophysiological phenomena visible in EEG signals with frequencies above the usual clinical range of analysis, so called Berger bands [10]. Since their initial description in 1992 [23] HFOs have been intensively studied as biomarkers of epileptogenic tissue and as signs of cognitive functions.

3.1 High-frequency oscillation characteristics

HFOs were first described in hippocampus of freely behaving rats as a physiologic phenomenon. They were named ripples with their frequency band ranging from 80-200 Hz [23]. Later, the same group of scientists described another type of HFOs in epileptic rats which were called fast ripples due to their high frequency bands 200-600 Hz. This early investigations led to the first human wide bandwidth recordings. Similar to the model of epileptic rats both ripple and fast ripple oscillations were identified in human epileptogenic hippocampus. A typical HFO appearing in iEEG signal is depicted in Figure 4 [10].

It should be noted that HFO definition as well as the definition of ripples and fast ripples, which is crucial for creating a gold standard dataset and development of automated algorithms, varies in literature. The duration of HFOs is often defined as a short transient event without any further specification of duration or only as duration range in a broad frequency band. However, some studies do mention HFO duration in number of cycles, 5 to 15 oscillations [23]. The frequency bands in which HFOs are defined also differ in publications, 80 – 500 Hz [23, 24], 100 – 500 Hz [25, 26], 100 – 600 Hz [27], 100 – 800 Hz [28]. Due to this vague definition, it is hard to make valid comparisons across studies and HFO detection algorithms since each of them was developed for detection of slightly different graphoelements.

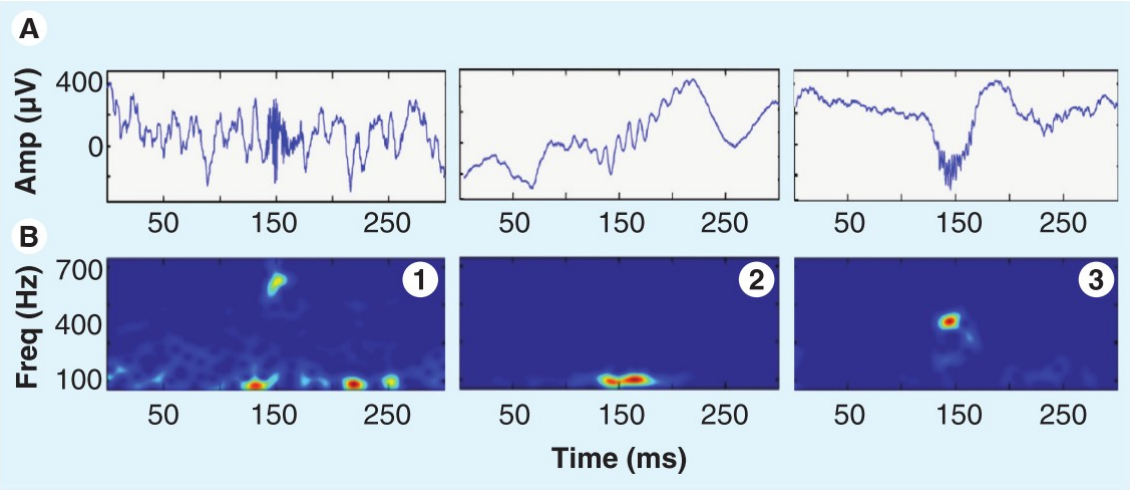

Figure 4: ***Representative examples of HFOs.***

Each plot shows two views of HFOs in 300ms window: (A) unfiltered iEEG with an HFO located in the center ~150 ms, (B) spectrogram (2.6 ms window). (1 & 3) Typical HFOs in fast ripple range. (2) Typical HFO in ripple range. Amp: Amplitude, Freq: Frequency [10].

Some recent studies also suggest that HFOs are occurring at frequencies above the FR range (> 1000 Hz), labeled ultra- or very-high frequency oscillations, but are deemed to be a different pathophysiological phenomenon [29].

3.2 Current state of HFO research in cognition

Ranging from 80 to 600 of cycles per second, HFOs are likely to bridge the local action potential firing of individual neurons with the large-scale interactions of neuronal networks. HFOs are, therefore, increasingly recognized for their potential to complement the animal studies of single-unit mechanisms underlying cognition and the human cognitive experiments using non-invasive imaging techniques [30, 31].

Studies of HFOs in cognition have largely focused on frequencies of the gamma range up to 120Hz which overlaps with the reported ripple frequencies. They are induced in the sensory as well as higher order processing areas, driven by bottom-up and top-down mechanisms, respectively, and have been associated with formation of perceptual and memory representations in humans[32]. Nevertheless, neuronal

interactions are known to extend beyond the classic gamma oscillations, e.g. synchronous firing of neuronal populations was shown to correlate most strongly with the 80-200Hz frequencies [33].

Much less is known about the roles of HFOs in the ripple, fast ripple and novel very high-frequency oscillations bands (125-1000Hz) during cognition. The underlying mechanism of ripple is believed to be discharges of synchronized firing between specific neuronal ensembles, mainly occurring during states of rest and sleep [23]. In sleep, ripples were shown to comprise sequential firing of specific hippocampal assemblies that were active during preceding behavior in rats [34]. This 'replay' of activity, observed also in reverse order and during quiet wakefulness, was initially proposed to underlie memory consolidation but recent evidence suggests an active role in decision-making [35]. Interestingly, ripples were shown to be generated by the same neuronal networks and mechanisms as the gamma oscillations [36]. Whether the human ripple-frequency HFOs support the same function as the hippocampal sharp-wave ripple complexes in rodents remains to be established, as well as the role of cortical oscillations in the ripple frequencies. At least one study suggests involvement of rhinal cortical ripples in human memory consolidation [37].

Network oscillations recorded in the highest fast ripple band of HFOs (250-1000Hz) were so far predominantly associated with pathological network activity in epilepsy [10, 38, 39]. Increasing evidence, however, suggests existence of physiologically-induced HFOs beyond the gamma and ripple bands reported in human behavioral tasks [40]. The role of these fast ripple HFOs in brain functioning remains to be explored, as is their relationship to the well described gamma and ripple oscillations.

3.3 Current state of HFO research in epilepsy

HFOs have been investigated in number of human studies, all of which confirmed the link between higher HFO rates and pathologic brain [38][25][41][26][42][24][43][44][45][46]. Unlike spikes, which are deemed to be another less specific biomarker, HFOs have been proven to better localize pathological tissue [24]. Studies investigating the relation of post surgical persistent seizures and areas with present pathological HFOs showed a better surgical outcome when the area

of the brain with HFOs was resected [47][48]. All of these studies, however, evaluated HFOs only in limited number of patients (~10) and/or reviewed only short segments of iEEG which lowers their statistical power. Most of the studies are also based on visual identification of HFOs which is a time consuming process, can introduce human bias into the results and is not feasible for large data sets. Lastly, results of HFO studies are often reported relative change of HFO rate in SOZ rather than absolute HFO rates which are not suitable for prospective studies, thus cannot be translated into clinical environment.

It has been proved that HFOs are also a physiologic phenomena naturally occurring in normal brain and are believed to be important for consolidation of memory [23][38]. The ability to distinguish between pathologic and physiologic HFOs might further improve localization of pathologic tissue. Nonetheless, it still remains unclear how to distinguish between these types of HFOs [39] even though some studies laid solid foundations for achieving this goal.

Another factor influencing HFO rate are different anatomical structures of the temporal lobe. The hippocampal structures are known to be more epileptogenic than others and they have been also proved to produce physiological HFOs [23]. Even though these facts are well known, most of the studies evaluate HFO rates in only one structure or disregard brain structures altogether.

Some attention has been given to the relation of HFOs and the behavioral state of the patient. Changes of HFO rates have been reported both during cognitive stimulation and during slow wave sleep [49][50][44]. The cognitive stimulation tasks, inducing cognitive processing in the brain, such as the odd ball task or picture presentation have been proved to reduce pathological HFOs and epileptic activity [40] whereas the slow wave sleep rises the HFO rate in the epileptic lesion [44].

4 DETECTION OF HIGH-FREQUENCY OSCILLATIONS

4.1 Why is objective HFO detector needed?

Even though HFOs have been studied for over a decade a clear definition of HFOs is still to be determined. For this reason, expertly reviewed HFOs are considered to be a gold standard. Nonetheless, this approach remains a flaw in the current methodology. Not only is the detection of HFOs based on subjective visual review inevitably biased but the inter-reviewer concordance can be poor [51]. Moreover, visual detection is a time consuming process which does not allow for implementing this approach for big data sets or online detection in OR. This methodological weakness could be overcome by implementing a reliable automated HFO detection and thus achieving consistent and objective results.

Apart from removing human factor from the HFO detection the ability to distinguish between particular HFO types is needed to achieve better localization of pathological tissue and to broaden the knowledge about the relationship between HFOs and cognition, behavioral states and anatomical structures. To date the main HFO separation was based on their frequency and amplitude. So far, as mentioned in section 2, separation into two groups based on frequency has been accepted. One group of HFOs was named ripples (80-200Hz, amp) and the second fast ripples (200-600Hz, amp)[23]. While this distinction is sufficient for some areas of the brain the underlying mechanisms of pathological and physiological HFOs still remain unclear and may vary in different brain structures and behavioral states. Another possible distinctions may be based on different features as in [52, 53].

4.2 HFO features

Generally the detection of a graphical element in a signal requires definition of its features. The features can differ significantly based on anatomy or whether the tissue is pathologic or not [52].

The three most obvious and most common features used in EEG processing are amplitude, duration and frequency. HFOs are a short-duration, high frequency events standing out from the background so all these features can be utilized for their detection.

Amplitude is often calculated from filtered signal, that has been further processed by for example root mean square sliding window or Hilbert transform and usually normalized. Such amplitude calculation is indirect and relative to the surrounding signal. An approach to calculate the amplitude of the event is during the post processing stage once the HFO is detected. The detection can be linked back to the raw signal and absolute amplitude in μV can be calculated. This value reflects the underlying biophysical processes more precisely than relative amplitude but can be influenced by noise, reference electrode and etc.

HFOs are wave like graphical elements. Thus, their frequency is linked to their duration through number of cycles. The definition of how many cycles an HFO should have is unclear since it varies in literature, especially the lower boundary.

Apart from the features resulting from the basic characteristics of the signal, additional, more complex, features can be estimated. These features are numerous but in general they often utilize either amplitude ratios, comparisons of parts of frequency spectra or signal entropy (see section 4.3).

4.3 HFO detectors developed to date

As a result of unclear HFO definition, the detectors designed by different groups are optimized using different filter and threshold settings according to their own definition of HFO. However, every detector designed to date utilizes a method that preprocesses the signal by applying frequency filters, calculates the energy of the filtered signal and pick candidate events as those exceeding the set statistical threshold.

Such assumption is correct for the most data sets. Nevertheless, it might fail in very active channels such as those located in seizure onset zone (SOZ) of epileptic tissue, where normalization of the signal can lead to lower sensitivity due to very high incidence of HFOs, therefore only HFOs with high energy get detected. Contrarily, in low active channels, such as those in white matter, the signal normalization can have the exactly opposite effect and result in lower specificity by detecting false positive events because only slight changes in signal power can exceed chosen threshold. Possible solution is to detect baseline segments ("*segments with no oscillatory activity of any kind*") and determine the statistical thresholds based on these segments [54].

The sensitivity and specificity of HFO detectors is often defined on gold standard detections produced by visual review but the approaches of calculation vary. Some authors detect HFOs with very low threshold to achieve 100 % sensitivity. These detections are then accepted or rejected by reviewers. This approach is problematic because it creates a bias in favor of the detector. Another approach is to manually mark HFOs without any previous detection. In this case the reviewers are blinded to HFOs detected by the detector but the definition of true negative instances becomes an issue. A possible solution is to mark inter-event intervals as negatives but this usually leads to very low specificity of the detector. Due to these differences, sensitivity and specificity from different works cannot be directly compared.

The characteristics of detectors are chronologically listed below according to the groups that developed them. A comprehensive summary is in Tab. 3.1.

Staba et al. [2002]

The detector designed by Staba et al. adopted the moving average of root mean square of the preprocessed signal as the energy metric [41]. The preprocessing stage involves band-pass filtration of iEEG signal (100-500 Hz). The metric threshold was set to 5 standard deviations above the mean of the whole signal. Events shorter than 6ms were disregarded and events less than 10ms apart were regarded as one HFO. The reported sensitivity of this algorithm was 84 %. The algorithm was originally developed for micro-electrode recordings in rats and humans.

Nelson et al. [2006]

Nelson et al. [55] suggested a detector using the energy metric called Teager energy which was initially designed for applications in acoustics [56]. In their experiment the signal was filtered by a Butterworth filter, however, the cut off frequencies were not reported even though the frequency setting is crucial. No sensitivity or specificity results were provided. The Teager energy metric was suggested for rat micro-wire recordings.

Gardner/Worrell et al. [2007]

Gardner et al. [51] developed a detector based on line length of the iEEG signal originally designed for detection of high-gamma events and subsequently used for HFOs [42]. In the preprocessing stage the signal was filtered by a Butterworth band pass filter (30 – 100 Hz [51], 80 – 1 kHz [42]). The statistical threshold was set to 95 percentile of the given statistical window (3 minutes). The sensitivity of this detector was reported to be 89.5 % [51]. The recordings for which this detector was designed were micro as well as macro-electrode human iEEG [51].

Crepon et al. [2010]

Amplitude envelope of filtered iEEG signal calculated by Hilbert transform was used in semi-automated detector designed by Crepon et al. [46]. The band pass filter used in preprocessing was set to 180 – 400 Hz. Putative HFOs were detected as 5 SDs of iEEG signal amplitude. The detector was developed for HFO detection in human macro-electrode depth and strip recordings.

Zelmann et al. [2010]

In contrast with the previously described algorithms Zelmann et al. [54] created an algorithm that uses previously detected background activity to calculate the signal statistics rather than considering signal surrounding HFOs as background. The filter settings were confined to the band pass 80-450 Hz. The threshold for putative HFO

detection is calculated as the 95 percentile of the cumulative distribution function of the previously detected background segments. The reported detector sensitivity was 96.8 +/- 8.91 % and specificity 99.1 +/- 8.91 %. The target recordings were human macro-electrodes.

Dümpelmann et al. [2012]

A detector based on some of the metrics used in previous works. The detector aims on detection in ripple band only, meaning that the frequency band in which it operates is 80 – 250 Hz. It utilizes signal energy, line-length and instantaneous frequency. These metrics are processed by a radial basis function neural network. The reported sensitivity was 49.1 % and specificity 36.3 % [57].

Lopez-Cuevas et al. [2013]

An online detector proposed by Lopez-Cuevas et al. [58] uses metric of signal complexity (Approximate entropy [59][60]) rather than signal energy. After calculation of approximate entropy of raw signal an artificial neural network was trained to detect HFOs with 4 neurons in the initial layer using last 4 values of approximate entropy as their inputs. This algorithm was designed for micro-electrode rat recordings.

Sahbi-Chaibi et al. [2013]

The algorithm designed by Sahbi-Chaibi et al. [61] uses part of Hilbert-Hunag transform and its integral part empirical mode decomposition (EMD) for HFO detection. Firstly the intrinsic mode functions (IMFs) are acquired using EMD. Instantaneous frequency and amplitude is calculated in each IMF with Hilbert spectral analysis. Because instantaneous frequencies are sensitive to noise, smoothing is applied to circumvent this drawback. Subsequently instantaneous amplitude coefficients are accumulated only in function of IMFs traces presented in HFOs band 80-500 Hz. The obtained 1-D signal is smoothed by root mean square operation and thresholded for detection of HFOs.

Birot et al. [2013]

A method for detection of FR in iEEG. The authors use frequency band of 256 – 512 Hz, which was chosen for methodological reasons. First, the signal energy is obtained by calculating line-length. After thresholding, the putative HFOs are further processed by either Fourier transform or wavelet transform, where the ratio between FR frequency band and lower frequency band is calculated. This metric is further thresholded and the final HFO detection is obtained. The reported sensitivity and specificity were not reported, however, the best AUC achieved was reported to be 0.983 and 0.986 for the Fourier transform method and wavelet transform method respectively. [62].

Burnos et al. [2014]

An HFO detector designed to detect in both ripple and fast-ripple frequency range. During first stage of the algorithm the signal is filtered and amplitude envelopes are calculated using Hilbert transform. Such signal is thresholded with low threshold setting to detect putative HFOs with high sensitivity. The putative HFOs are further processed by Stockwell transform. The power spectral density was used to distinguish between HFO detections and putative detections produced by Gibb's phenomenon, such as artifacts and spikes [63]. The sensitivity and specificity was evaluated for each recording separately, and average values were not calculated.

Study	Freq range [Hz]	Used technique	Sensitivity	Specificity	Target recordings
Staba et al.	100-500	RMS	84.0%	-	Micro/human
Nelson et al.	-	TE	-	-	Micro/rat
Gardner/Worrell et al.	30-100/80-1000	LL	89.5%	-	Micro,Macro/human
Crepon et al.	180-400	AE	-	-	Macro/human
Zelmann et al.	80-450	MNI	96.8%	99.1%	Macro/human
Dümpelmann et al.	80-250	RMS + LL + IF	49.1%	36.3%	Macro/human
Lopez – Cuevas et al.	-	Aent	-	-	Micro/rat
Sahbi-Chaibi et al.	-	HHT	90.7%	-	Macro/human
Birot et al.	256-512	LL + FFT/WT	-	-	Macro/human
Burnos et al.	80-500	AE + PSD	-	-	Macro/human

Table 1: ***Overview of HFO detectors.***

Used techniques abbreviations: RMS – root mean square, TE – Teager energy, LL – line-length, AE – amplitude envelope, computed by Hilbert transform, MNI – baselane based detection, IF – instantaneous frequency, Aent – approximate entropy, HHT – Hilbert-Hunag transform, FFT – fast fourier transform, WT – wavelet transform, PSD – power spectral density.

As it is apparent from Table 1, the detectors that have been designed vary in frequency ranges, the target recordings and used technique. Even when evaluating sensitivity and specificity the authors of the listed detectors vary in definition of true positive and true negative detections which makes the detectors impossible to compare. A comparison has been attempted by Zelmann et al. [64] and it was found that each detector has to be optimized on certain type of data and re-validated in order to function properly making wide-spread application of any of these detectors impossible.

5 AIMS OF DISSERTATION

The main goal of this work was development and validation of automated HFO detectors, study of HFOs in patients suffering from intractable epilepsy and localization of epileptogenic zones within pathologic brain. Apart from the main focus on automated detection algorithms, HFO occurrence analyzes were carried out and result presentation tools were created within this work. The main analyzes and methods that may in the future contribute to basic research of the brain as well as improved diagnostics are listed below:

- Fast and robust algorithms for detection of high-frequency oscillations and their validation with regard to gold standard data sets as well as SOZ and resected area in patients with good surgical outcome.
- Modular software tools to validate any HFO detection algorithm.
- Characterization of HFOs with regard to the behavioral state of the patient, anatomical structure, type of epilepsy, etc.
- Software tools to detect HFOs close to real-time detection with a lag approximately 10s make it possible to view HFO occurrence inside the operation room to evaluate the feasibility of such approach to map and resect the epileptogenic focus in one procedure.
- Tools to present HFO occurrence in a comprehensive form for physicians.

The ultimate gold of this work is to provide physicians with additional information about HFO occurrence, and thus, better localize pathological tissue in patients with pharmacoresistant focal epilepsies and improve the outcome of the brain surgery, therefore life and well-being of the patients.

6 DATA CHARACTERISTICS

This section describes the data used in this thesis. Because the data come from two institutions – St. Anne's University Hospital in Brno (FNUSA) and Mayo Clinic – Mayo Systems Electrophysiology Lab (MSEL), each sub-section is accordingly divided and describes the different characteristics.

6.1 Subjects

The data comprised of recordings from patients with medically intractable focal epilepsies who underwent electrode implantation to localize seizure foci prior to surgical resection. All subjects were on anti-epileptic drug medication (AED) which was reduced for the purposes of video-EEG monitoring. Written consent was obtained from each patient prior to the study.

6.2 Recording devices and electrodes

Recording devices both in FNUSA and at Mayo Clinic were certified medical devices for video-EEG monitoring.

In FNUSA, ALCIS electrodes were used for intracranial invasive exploration. Individual electrode sizes and types were determined by clinical requirements. Acquisition device (Brainscope - BioSDA09 / 192ch) is capable of simultaneous recording of up to 192 channels. It utilizes 24 bit A/D converter per channel and all channels are sampled at 25 kHz. The dynamic input range of +/- 20mV with 10 nV resolution.

In MSEL the used electrodes were Ad-Tech subdural grids, strips and depth electrodes. Subdural electrodes had varying number of contacts depending on the clinical needs. A scalable (32–320 channels) acquisition platform capable of continuous long-term recording was used (Neuralynx Inc.). The Digital-Lynx system uses an individual, high resolution, 24 bit A/D converter per channel to directly digitize the

electrode signal using a single, DC-coupled, low noise differential amplifier and anti-aliasing filter (low pass 9kHz). All channels are simultaneously sampled at 32kHz with a DC to 8kHz signal band- width. This high resolution design provides a dynamic input range of ±132mV with 1V resolution (18th bit).

6.3 Data collection and manipulation

While the patients in both centers had similar diagnoses and were admitted into hospital to undergo iEEG monitoring the data collection differs based on both historical needs and practices as well as technical possibilities of both institutions.

In FNUSA the data used in this work consisted of two sets. First, the resting state recording was acquired when patient was lying still without any auditory or visual stimulation. Each recording was approximately 30 minutes long. Second, the oddball paradigm, which includes visual stimulation with letters and requires patient's response.

In MSEL the recorded data were acquired during the patients' stay in intensive care unit (ICU). The length of the recordings differs as it was dependent on the length of patient's stay at the ICU and on patient's current clinical state. Two tasks were done by some of the patients. A motor task which consisted from on screen instructions and patient's response by finger movements. And picture presentation task involving presentation of emotionally affective charge.

After acquisition, the iEEG signals were filtered and downsampled to 5 kHz sampling frequency for processing and storage reasons. Since the analyzed frequency bands reach maximum of 1 kHz the sampling frequency satisfied Nyquist's theorem by a large margin.

Detections and recording meta data, such as signal quality, anatomical location of individual contacts and channels from which seizures propagated were stored in MySQL database for fast and modular processing.

7 DEVELOPED AND IMPROVED ALGORITHMS

Three detectors of HFOs were used within the frame of this work. Each of the detectors was developed for different definitions of HFO and distinct purposes. This section is divided into three chapters each describing the algorithms, their purposes, advantages and disadvantages. All HFO detection algorithms can generally be divided into three stages: pre-processing, detection, post-processing. All of these stages are described in individual sub-sections. To demonstrate the core principals of each algorithm, all figures utilize the same example data with one HFO on a sharp transient – interictal epileptiform spike (Figure 5).

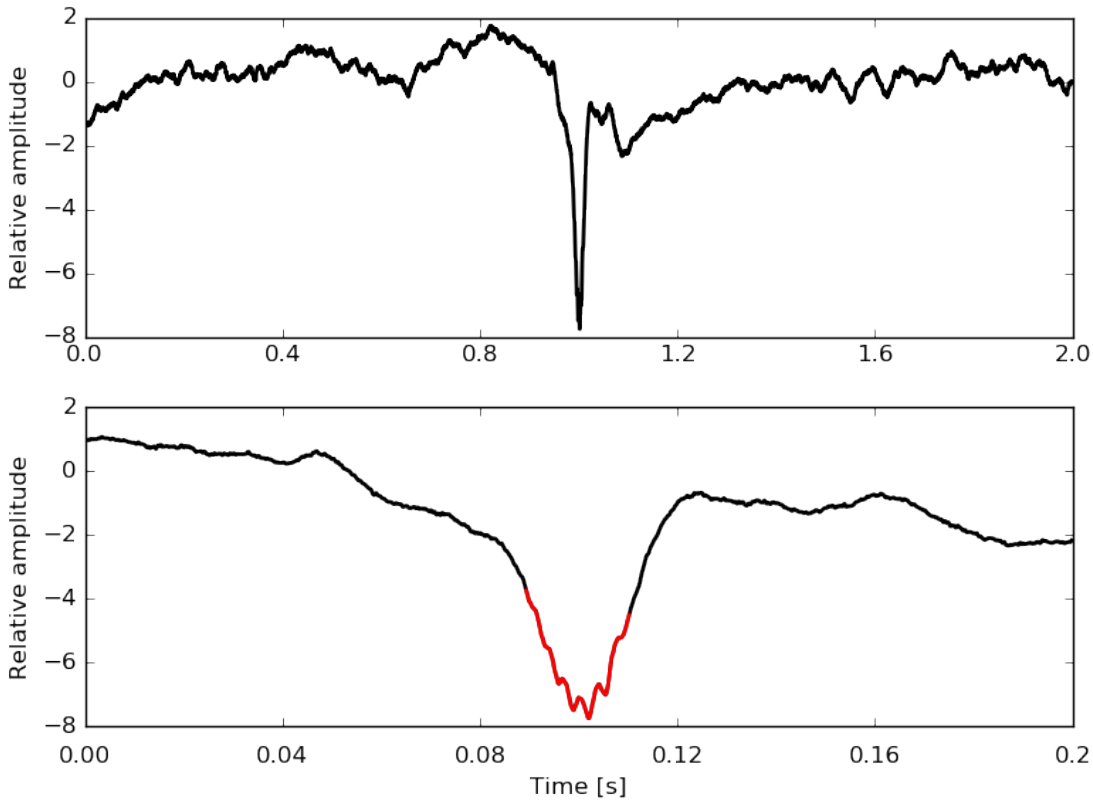

Figure 5: ***Sample signal.***

Top – raw iEEG signal (2 seconds) with a spike and HFO on its peak. Bottom – zoom of the signal from the top pane. HFO marked in red.

7.1 Ideal HFO detector

There are several characteristics which an ideal HFO detector should have. This definition stems from requirements of clinical practice, processing time and detector portability in different centers.

First, the detection itself should achieve the sensitivity and specificity close to 100 %. While this condition seems unrealistic the values close to 100 % can be achieved depending on the method of metric calculation. This problematic is further described in section 8.1.

Second, the algorithm should require as little of fine tuning as possible. This means, there should be a limited number of thresholds that are needed to be set. Algorithms with many thresholds usually need to be tuned and adjusted do particular data sets and cannot be uniformly applied for different signal types and recordings with varying characteristics, such as sampling frequency, signal-to-noise ratio, dynamic range, etc.

Third, the processing time should be as short as possible while needing as little of processing power and memory as possible. There is, of course, a connection between the processing power of the unit and the processing time, nonetheless, the detector should be usable on standard desktop PCs in order to be usable across institutions in the world.

Last but not least, an ideal algorithm should be multiplatform and available for no additional costs, to be easily usable by any epileptic center. Meaning that the program should be written in one of the cross-platform languages (C, C++, python, Java, etc.) and it should not require any third-party commercial software, such as Matlab.

7.2 Line-length detector with feature cascade

This algorithm was developed to analyze enormous data sets produced by long term clinical iEEG recordings (TB of data). The main purpose was to retrospectively evaluate the relationship between the pathological brain and HFO rates recorded with

iEEG electrodes. The core of this algorithm, i.e. the processing part was developed by Benjamin H. Brinkmann (MSEL). The main advantage of the line-length metric is that it reflects increases in both signal amplitude and frequency. However, it is dependent on sampling frequency and prone to presence of noise in the signal. The algorithm was already used in number of works [51, 62, 64, 65].

In the pre-processing stage the signals are usually visually checked for excessive noise levels or even channels that include no useful signal. These channels are excluded from the analysis. The rest of the channels are filtered with a band-pass 4-pole butterworth filter to 100-600 Hz frequency band. In the detection stage a 10s statistical window is created and the filtered signal is converted to line-length signal (Equation 1), using 50ms (5 oscillations at 100 Hz) sliding window with ¼ overlap. These parameters can be varied as needed. Mean and standard deviation are calculated and a fraction of standard deviation above the mean is used as a threshold. The threshold is set so that the sensitivity of this step is 100 %. The LL metric of a filtered signal is demonstrated in Figure 6. The possible danger here is that if signal-to-noise ratio is low, the noise can increase overall line-length metric and the HFO is not detected because it does not stand out from the background. Conversely, if the threshold is set too low, the signals that are less active yield more detections than active channels. This happens due to higher line-length standard deviation in active channels.

$$\mathrm{LL} = \sum_{k=t-N+2}^{t} \left| (x_k - x_{k-1}) \right|$$

Equation 1: Line-length metric.

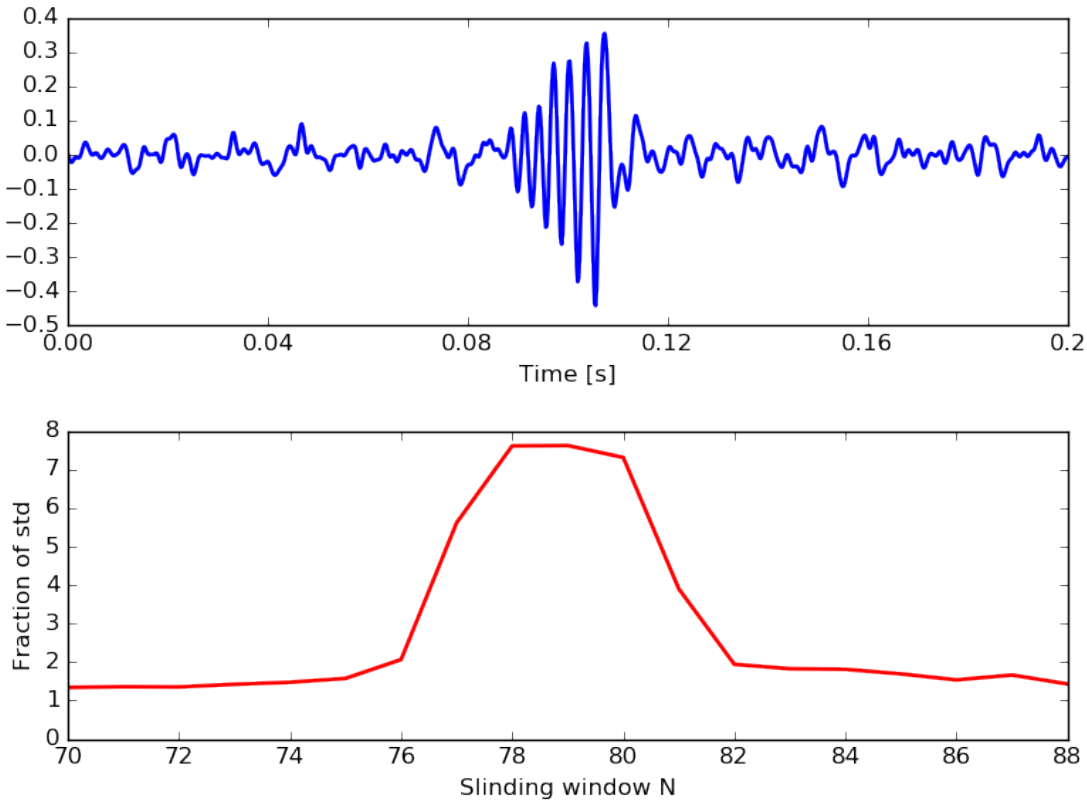

Figure 6: ***Line-length metric.***

Filtered signal with corresponding line-length metric (100 ms sliding window with 25 ms overlap). Top – filtered signal (80 – 600 Hz). Bottom – Line-length metric.

The post-processing stage was added within this work and it involves calculation of HFO features – duration, amplitude, frequency (using multi-taper power spectral density) and event to background ratio and correlation with low-passed signal for improvement of algorithm specificity. The detection process is represented by the diagram in Supplement 1.

7.2.1 Advantages of the algorithm

The main advantage of the line-length algorithm is its speed (~5 minutes/channel/2 hours of recording at 5 kHZ sampling rate) which makes it a good tool for processing large data sets. Moreover, the computed features may be further used for data mining tasks and to develop more sophisticated classifiers.

7.2.2 Disadvantages of the algorithm

While this algorithm is fast, the detection characteristics are far from being ideal (see section 8). This is likely caused by Gibb's phenomenon which is not accounted for. Nevertheless, it is suitable for analysis of very high frequencies (> 500 Hz) in a high quality noiseless signals where Gibb's phenomenon is less likely to influence detections. If these conditions are met, the line-length detector can provide useful information.

7.3 Algorithm based on frequency homogeny

The purpose of this algorithm was to be able to process large datasets while improving specificity compared to less sophisticated methods. Originally designed by Mathew Stead (MSEL) the algorithm efficiently removes false positive HFO detections that occur due to Gibb's phenomenon while maintaining reasonable speed of detection.

In the first step the signal is filtered with band pass butterworth filters in a sequence of overlapping frequency bands that cover the whole frequency span of high-frequency oscillations (80 – 600 Hz). Each filtered band is processed separately in the subsequent steps in the same fashion.

First, the amplitude envelope of the filtered signal is calculated using Hilbert transform (Equation 2, Figure 7).

$$F(t)=\frac{1}{\pi}\int_{-\infty}^{\infty}\frac{f(x)}{t-x}dx$$

Equation 2: Hilbert transformation.

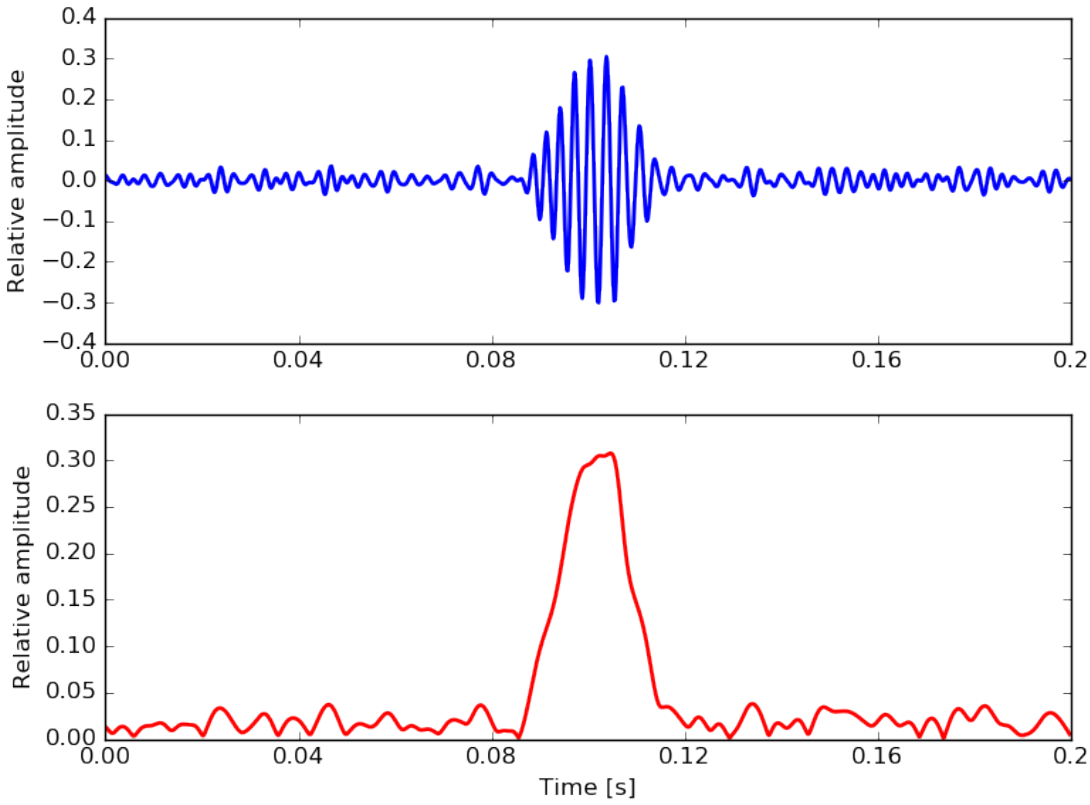

Figure 7: ***Amplitude envelope metric.***

Top – filtered signal (237 – 332 Hz) in one of the frequency bands utilized in the frequency homogeny algorithm. Bottom – amplitude envelope of the filtered signal.

Second, a metric evaluating frequency stability is calculated as the "signal-to-noise" ratio (Equation 3). The numerator of the equation is the root mean squared cosine representation of the narrow-band signal phase (Equation 4) and the denominator is the root mean squared difference between the cosine representation of the broad-band and narrow-band filtered signal phases (Equation 5). The broad-band filtered signal has the same cut-off frequency as the narrow-band passed signal but the low cut-off frequency is four times smaller (Figure 8). This second metric servers for elimination of detections caused by higher amplitude in filtered signal which is produced by Gibb's phenomenon.

$$SNR_j = \frac{\sqrt{npxx_j}}{\sqrt{bpxx_j}}$$

Equation 3: Frequency homogeny metric.

where

$$npxx_j = npxx_{j-1} - np_i^2 + np_k^2$$

Equation 4: Frequency homogeny numerator.

and

$$bpxx_j = bpxx_{j-1} - (bp_i - np_i)^2 + (bp_k - np_k)^2$$

Equation 5: Frequency homogeny denominator.

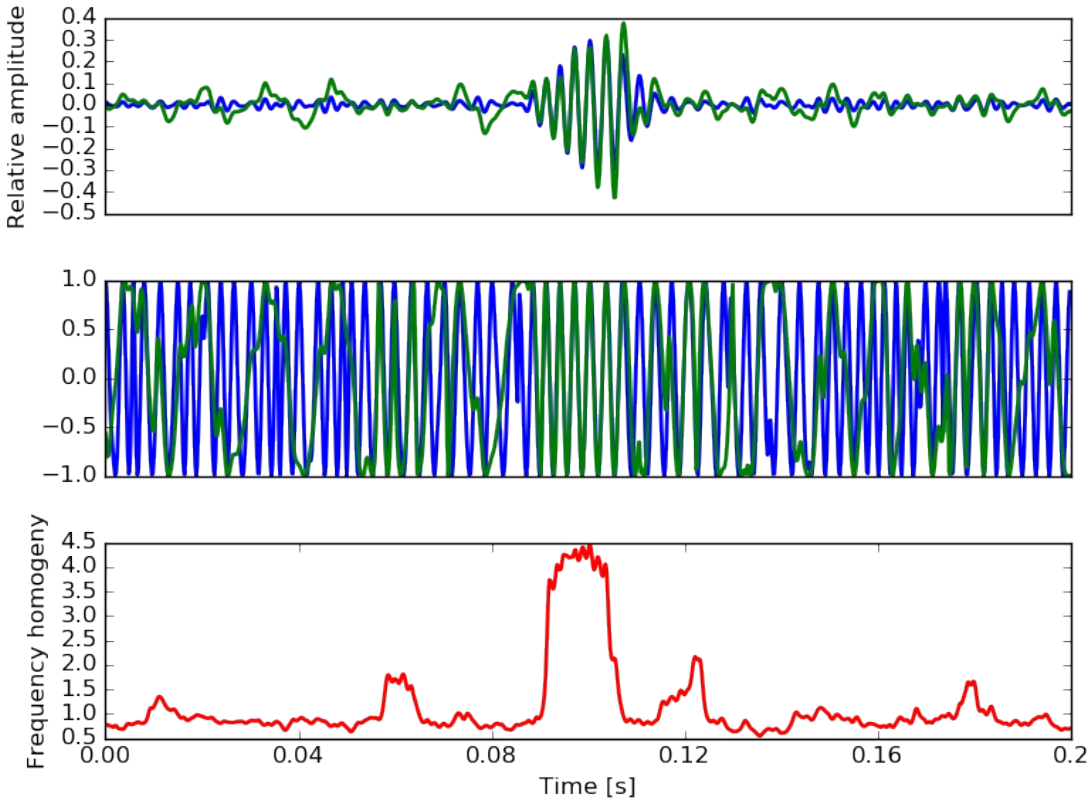

Figure 8: ***Frequency homogeny metric.***

Top – blue: narrow band passed signal (237 – 332 Hz), green: broad band passed signal (59 – 332 Hz). Middle – cosine transformed signals from the top pane. Notice the synchronization around the HFO area. Bottom – frequency homogeny metric.

The third step of metric calculation consists of calculating the dot product of the normalized signal amplitude envelopes and frequency stability metric, thus obtaining a signal that utilizes both amplitude and frequency features of the analyzed signal. If one of the metrics is negative the resulting signal is put to 0 (Figure 9).

To account for non-stationary character of EEG signal all metrics are normalized by Poisson normalization. The detection of putative HFOs is done by thresholding the normalized product metric. Each putative HFO enters the cascade of minimum and maximum value boundary thresholds for amplitude, frequency stability, dot product and duration. The thresholds are calculated from cumulative distribution functions that were generated from the features of HFOs visually marked by expert reviewers. The block schema representing the algorithm can be found in Supplement 2.

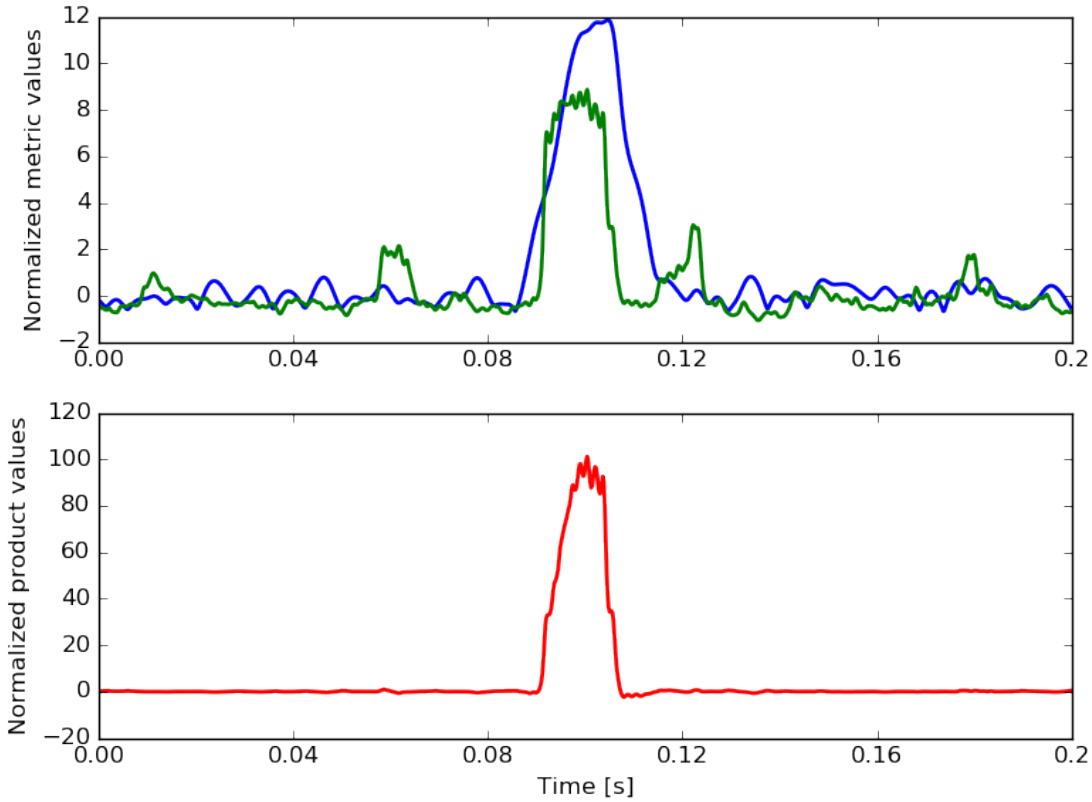

Figure 9: ***Dot product metric.***

Dot product metric is produced by sample by sample multiplication of amplitude envelope and frequency homogeny metrics. Top – blue: normalized amplitude envelope metric, green: normalized frequency homogeny metric. Bottom - dot product metric.

7.3.1 Advantages of the algorithm

The main advantage of this algorithm lies in the effective elimination of Gibb's phenomenon that occurs during filtration of a sharp wave and therefore increased specificity of detection. The algorithm is fast enough for real time detection.

7.3.2 Disadvantages of the algorithms

While the speed is sufficient for real time processing of iEEG signals, detection run on very large datasets is slow compared to the line-lengh detector. Another disadvantage is the rigid threshold setting created based on gold standard detections. This makes the algorithm less usable on different datasets. To eliminate this effect the thresholds have to be calculated again on the gold standard detection dataset.

7.4 Hilbert 2D detection algorithm

The algorithm was developed to detect physiological HFOs occurring during cognitive and memory tasks and to broaden the understanding of pathological HFOs with regard to their features. The aim of this algorithm is to provide detailed study of individual pathological and physiological HFO features, and thus contribute to the distinction between the two groups and their behaviors.

Instead of using a wider frequency band of interest, such as 80 – 600 Hz this algorithm uses a series of band passed signals using 4-pole butterworth filter. This can be achieved by band-passing the original signal with 1 Hz step. Z-score for each signal is calculated. (EQ) Such approach can be visualized in a time-frequnecy matrix (Figure 10). This matrix differs from classical time-frequency analysis in three aspects. The produced matrix does not use sliding windows so each sample corresponds exactly to the sample of raw signal. Furthermore, each band reflects changes in amplitude rather than power of the band, result of which is that baseline noise, such as 60 Hz, is not visible in the matrix. Finally, the 1/f characteristic of EEG is overcome by individual z-score normalization of each band.

$$\text{z-score} = \frac{x - \bar{x}}{s_x}$$

Equation 6: Standard score (z-score) calculation.

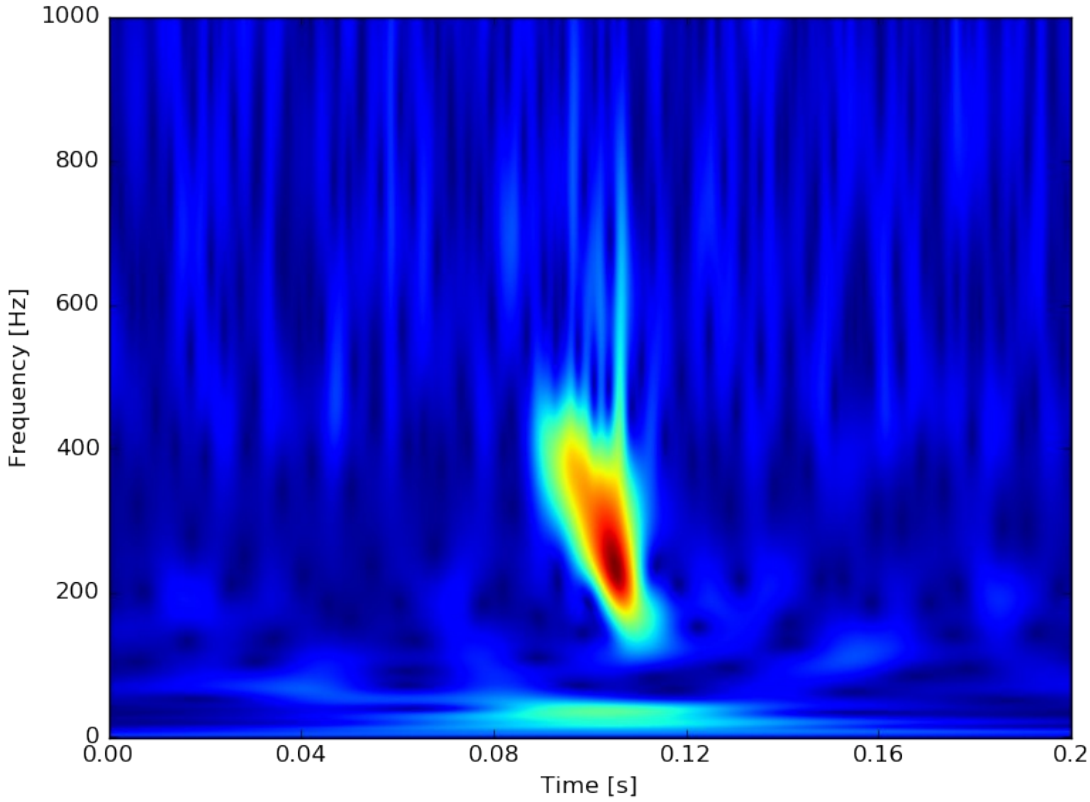

Figure 10: ***Time-frequency matrix of z-score amplitude envelopes.***

2 – D Representation of HFO in time-frequency matrix with 1 Hz frequency step.

As it is apparent from (Figure 10) the higher frequencies of the histogram carry redundant information. Therefore, choosing a logarithmically spaced frequency bands is a logical approach to reduce the information redundancy and increase algorithm speed. The logarithmically spaced equivalent is depicted in (Figure 11, top).

In order to overcome the consequences of Gibb's phenomenon the cross correlation is calculated between band-passed signal and the low-passed signal with the common high cut-off frequency. To speed up this calculation the relationship between convolution and correlation is exploited (Equation 7, Equation 8) and convolution is

done by multiplication in the frequency domain (Equation 9). The cross correlation signals can be again visualized in a matrix (Figure 11, middle).

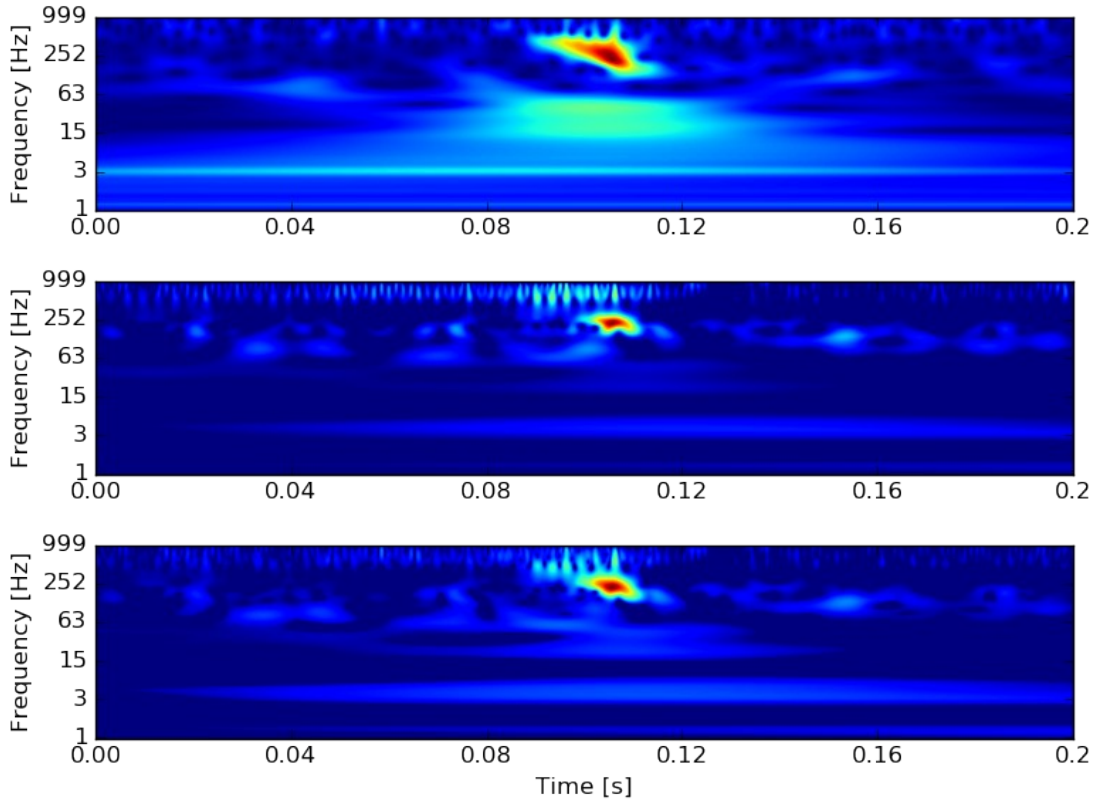

Figure 11: ***Time-frequency z-scored metric with cross-correlation, log spaced.***

Top – log spaced time-frequency z-scored matrix of amplitude envelopes, middle – cross-correlation between ban-passed signal and low-passed signal matrix, bottom – square root of the amplitude and correlation matrices. Notice the turquoise trace produced by Gibb's phenomenon in the top pane which is eliminated by using the cross-correlation metric.

$$corr\left(x[n],h[n]\right)=\sum_{k=0}^{\infty}h[k]x[n+k]$$

Equation 7: Correlation

$$x[n]*h[n]=\sum_{k=0}^{\infty}h[k]x[n-k]$$

Equation 8: Convolution

$$f(x) * f(h) = F(x) \cdot F(y)$$

Equation 9: Convolution in frequency domain.

To create a metric that takes into account both amplitude and cross correlation the square root of the dot product is calculated. The computed metric is depicted in the bottom pane of Figure 11.

The detection of events is done by thresholding the final metric in each frequency band. Since the metrics are z-scored, the used threshold represents a fraction of standard deviation above the mean. The detections with less than one cycle period apart in one frequency band are joined into one event. The detections in different frequency bands overlapping in time domain are joined into a single HFO detection.

Only one post-processing step is applied to reduce the number of false positive detections. The number of cycles is calculated using event peak frequency and duration and the events that are shorter than 1 cycle are discarded. The detections then enter a cascade of feature calculations. The block diagram of the algorithm can be found in Supplement 3.

7.4.1 Advantages of the algorithm

Precise feature calculation and the sensitivity level are main advantages of this algorithm. Features obtained by precise analysis can be utilized in post-processing and allow for more in depth analysis of detected HFOs.

7.4.2 Disadvantages of the algorithm

The main drawback of this method is the long processing time. Depending on sampling rate the processing time of one trial is ~5-10s which is close or above the real-time processing time. Another disadvantage is low specificity with regard to human scoring which can be partially overcome with post-processing steps by thresholding detections with computed features or by clustering the detections based on these features and using clusters as detections.

8 DETECTOR EVALUATION

To quantify the efficiency of HFO detection algorithms they have to be evaluated. Even though each publication of HFO detection algorithm method contains some form of efficiency quantification the methods for detection evaluation are not unified which makes a direct comparison almost impossible. This chapter discusses the problems of variable approaches to evaluation and presents the efficiency of algorithms included in this work.

8.1 Pitfalls of detector evaluation

As mentioned in section 3.1 the main problem of HFO detection is the lack of clear definition. This discrepancies in HFO definitions makes it difficult to mark HFOs uniformly across different institutions. Moreover, while human reviewed HFOs are considered the gold standard the marking of HFOs is inevitably a subjective process which results in poor inter-reviewer concordance. This problem is commonly overcome by submitting the same segment of data for review to multiple medical professionals. The HFOs marked by the majority of the reviewers are considered true positives.

Apart from the unclear HFO definition the recording equipment and methods differ from institution to institution. The differences in recording techniques and methods result in development of algorithms tailored to data and HFO definitions of individual institutions. Such algorithms are difficult to compare since they are tuned to a particular data set. A possible solution to this problem is to create an inter-institutional library of data segments with marked HFOs and resected tissue areas by multiple epileptologists and train the algorithms on these data segments. All algorithms would then be run and evaluated in the same fashion which would yield comparable result. The initiative to create detector library with common evaluation tools has been already started as an open source project (http://github.com/HFO-detect) which is maintained by the author of this work. The common evaluation and detection of shared datasets would lead to enhancement of algorithms and benefit patients.

8.2 Approaches to evaluation

Evaluation of algorithms depends on the desired output. In case of HFO detection algorithms the general standard is a comparison to a gold standard dataset marked by epileptologists. While this approach is generally accepted the inter-reviewer variability and subjectivity is a persistent problem.

Precision of HFO feature calculation is often disregarded, however, it can be used as an evaluation method in case the results of the detection are used for in-depth study or HFO clustering.

Another possible approach is to evaluate the detection based on the localization of pathological tissue. This method effectively eliminates the problem of unclear HFO definitions, however, can be influenced by detections that have different characteristics than HFOs, such as spikes.

8.2.1 Evaluation methods based on gold standard datasets

Traditionally the evaluation of a detection method is done by constructing confusion matrix for the method and calculating its sensitivity and specificity with regard to the ground truth. This approach is often used for example in evaluation of medical screening tests.

Since detection algorithms use thresholds for tunning their performance the receiver operating curve (ROC), developed by electrical engineers and radar engineers during World War II for detecting enemy objects in battlefields, appears to be an apt approach. The ROC analysis serves for determination of the optimal model or threshold with the best specificity and sensitivity that can be achieved. The quality of the model is usually expressed by the x and y values of the point closest to the [1,1] position in the ROC graph or by the area under the curve (AUC).

In case of an HFO detector ROC yields results that largely depend on the definition of a negative observation. HFOs are relatively rare event in iEEG signals so using a sliding window and evaluation for HFO presence results in true negative count significantly larger than other confusion matrix statistics. On the other hand, defining segments between gold standard detections as true negatives yields disproportional

counts of false positive detections compared to true negative detections. This phenomenon propagates into the calculation of ROC and produces seemingly excellent or poor results. The definitions of true negatives in scientific papers regarding HFO detection algorithms differ, making the comparison even more complicated. ROC curve is, therefore, not suitable for this evaluation.

The negative observation problem can be overcome by using the precision-recall curve. The curve is calculated using recall, which is an equivalent of sensitivity, and precision, which is the proportion of number of true positive detections to all positive detections. Contrary to specificity, precision does not include true negatives in its calculation. That leads to more realistic curve characteristics than ROC curve.

Another way to overcome the negative observation problem is to use error trade-off curve as the evaluation metric, which is not very common. Error trade-off curve plot contains false reject rate(FN / TP + FN) versus false accept rate (false positive rate – FP / TN+FP). The advantage in comparison to ROC, however, lies in the scaling of x and y axes. These axes are non-linearly scaled by their standard normal derivatives.

8.2.2 Evaluation of detectors with regard to HFO features

Features of individual HFOs might be a key to solve a number of problems regarding HFO detection and analysis. Precise feature estimation is, therefore, one of the desired attributes in HFO detection. HFO features can not only be useful in post-processing steps to enhance detection sensitivity and specificity but they may also contribute to distinction between pathological and physiological HFOs. Furthermore, HFO features may be variable both from temporal and spatial point of view which can be exploited in localization of epileptic foci as well as in seizure prediction.

One way to evaluate the precision of feature estimation is to compare the estimated value with a value produced by another method or a value estimated by visual review. However, all methods have some degree of error and visual review is prone to reviewer bias.

Another approach is to select a piece of iEEG signal without any high frequency activity and create artificial HFOs with known features. These values can then be compared with the values estimated by the detector and the error can be calculated.

The artificial HFO method can also be used to evaluate the error of human reviewers and compare inter-reviewer concordance as well as compare the results of human estimation with detector estimation.

8.2.3 Evaluation methods based on localization of pathologic tissue

Rather than relying on the unclear HFO definition and poor inter-reviewer detection reproducibility this approach directly evaluates the usefulness of the algorithm by correlating the number of detected event per channel with the pathology of the tissue surrounding electrode contacts.

Definition of pathological tissue may vary. Nowadays, pathological tissue in iEEG is generally defined as the first temporal onset of seizure in particular channels and so called irritative zone which exhibits interictal epileptiform spikes. Although successful to some extent, the resection of SOZ channels does not guarantee seizure freedom for patients which leads to search for other biomarkers. The only way of defining the pathological tissue correctly is to select patients with favorable surgery outcome and marking channels that were resected during surgery. However, surgical routines involve resection of whole structures, therefore, healthy tissue is resected too and it is unclear around which particular contacts was the pathologic tissue located.

The evaluation method can also exploit machine learning algorithms by clustering the detections, picking useful clusters which localize the pathological tissue and training a classifier to automatically classify detections into clusters in post-processing steps. To make the clustering possible HFO features have to be estimated. This can either be done in the detection process (algorithms 7.3, 7.4) or during post-processing (algorithms 7.2, 7.4). In order to achieve effective clustering the relevant features have to be selected. This step is often ignored in the literature and can potentially degrade the result of clustering.

The drawback of this method is the fact that the detected events that are used in evaluation can be a different electrophysiological phenomenon such as spikes and that the pathologic tissue can be incorrectly localized by neurologists. This, on one hand, can potentially lead to degradation of HFO usefulness as currently defined, on the other hand, can also lead to more precise definition of this biomarker.

8.2.4 Evaluation of algorithm speed

Algorithm speed is important both for research and clinic. In research, long processing times hinder subsequent analyzes. Nowadays results in clinic are delivered with delay of approximately 24 hours depending on the implemented algorithm. While this is currently sufficient, online or near online (~ 10 mins) implementation of algorithms is desirable in order to evaluate actual state of the patient's brain in operation room or intensive care unit. This could lead to higher patient comfort and shorter stay in hospital or to better medication management. On the other hand, faster and simpler algorithms are usually less precise which might not be apt for resection guidance.

While crucial for online implementation, algorithm speed is surprisingly disregarded in scientific papers. It is relatively easy to test by applying different algorithms to the same dataset but might vary on different computers and depends on the programming language.

8.3 Used evaluation methods

All three detectors were evaluated by the evaluation methods mentioned in the previous chapter. Since each detector was developed under slightly different conditions and for varied purposes the results acquired for the given data set might not correspond to the results when applied to data sets that have, for example, different montage.

8.3.1 Analysis based on gold standard data sets

Acquisition of the gold standard detections was done separately by two expert reviewers in iEEG signals from 5 minute segments in 3 patients. 9 channels per patient were evaluated; 3 channels were localized in SOZ, 3 in IZ and 3 in nonSOZ area of the epileptic brain which was previously selected by epileptologists in clinical recordings. The HFOs were marked as segments of filtered signals that had 4 times higher amplitude than the surrounding signal and the amplitude spanned at least 4 cycles. To eliminate false detection produced by filter ringing care was taken to review the detection in the raw signal for sharp transients. Only the detections where both reviewers agreed were considered true positives.

Evaluation was carried out for detected events without any correction and for detections where noisy segments were excluded from the analysis in semi-automated fashion.

Numbers of true positive, false positive and false negative detections were collected and precision-recall characteristics were calculated and plotted. Numerical evaluation was done by calculating F_1, F_2, and $F_{0.5}$ measures (Table 2).

8.3.2 Analysis based on feature estimation precision

To evaluate the feature estimation of the detectors, artificial HFOs were inserted into 20 minute long iEEG signal, which was previously visually checked for absence of visible HFOs. The used signal was taken from a contact located in white matter to avoid muscle artifacts and possible contamination by physiological HFOs from neocortex or structures of lymbic system. Furthermore, the signal was visually checked for any signs of pathologic activity and artifacts. The artificial events in form of simulated spikes, HFOs, delta functions, line noise and HFO-spikes (HFOs coincident with spikes), were inserted in 3 second intervals with varying amplitude, frequency and duration. To assess the influence of event amplitude on feature estimation the signals with artificial events were created for different amplitudes separately with the values spanning from 0.1 to 0.5 std (0.1 std step) of iEEG signal amplitude. In order to to investigate whether noise produces any distortion in feature estimation, separated analysis was conducted on signals with superimposed pink noise, which is typical for EEG. All algorithms were run with the lowest threshold settings to achieve the highest sensitivity possible.

This analysis is somewhat limited by the detection methodology. In case of the line-length detection algorithm the amplitude and frequency have to be computed in post-processing steps because it utilizes only one frequency band and the line-length metric takes both features into account. Frequency homogeny algorithm uses rigid frequency bands thus a priori creates error in the estimation of this feature.

8.3.3 Analysis of HFO rates with regard to localization of pathologic tissue

A sample of 30 minute recordings from 5 patients was processed by automated detectors developed and modified in this work. Clinical recordings were reviewed by experienced epileptologists and seizure onset zone, irritative zone and normal channels were marked. Irritative zone was marked within the channels that had clear pathologic activity. Determination of resected area and subsequent channel marking was done by experienced clinicians using overlapped pre and post-surgical MRI. Surgery outcome was evaluated based on Engel class. Four patients had favorable outcome of Engel IA while one had persisting seizures with outcome Engel IIIA.

The detection was done by all algorithms for varying threshold settings and best performing threshold was determined using the lowest p value (t-test). ROC for each detector was constructed using either SOZ, SOZ+IZ or resected channels as targets, the varying variable was HFO rate. To compensate for potential differences in patients the same analysis was done for per patient normalized rates. The AUC were calculated for each ROC separately to evaluate pathologic tissue localization.

8.3.4 Analysis of algorithm speed

All algorithms were run on one channel of itracranial EEG data with the length of 30 mins and 5 kHz sampling frequency. Standard desktop computer unit was used for evaluation with 12 GB RAM memory and Intel® Xeon(R) CPU E5-1620 0 @ 3.60GHz × 8 processors. Algorithms were all implemented in Python programming language.

8.4 Results

Automated HFO detection is a complex task that is still being actively developed. Individual detection methods vary in HFO definition, the purpose for which they were developed and the datasets on which they were tested. This makes the comparison across multiple institutions difficult. The detection methods created in this work do not suffer from these problems because they are tested on the same datasets and evaluated by uniform methods.

8.4.1 Results of comparison with gold standard detections

Construction of precision-recall curves proved that frequency homogeny algorithm achieved the best performance at detecting human scored events with the lowest F scores.

The performance of line-length detector proves the usefulness of this algorithm in HFO detection. The reasonable performance shows that this method is robust, albeit simple.

Hilbert detector exhibits poorest performance regarding agreement with gold standard detections.

Similar analysis with semi-automated approach, where noisy segments in the data were marked by reviewers and all detections in these areas discarded, was performed. All detectors showed improved performance (Figure 12, Table 2).

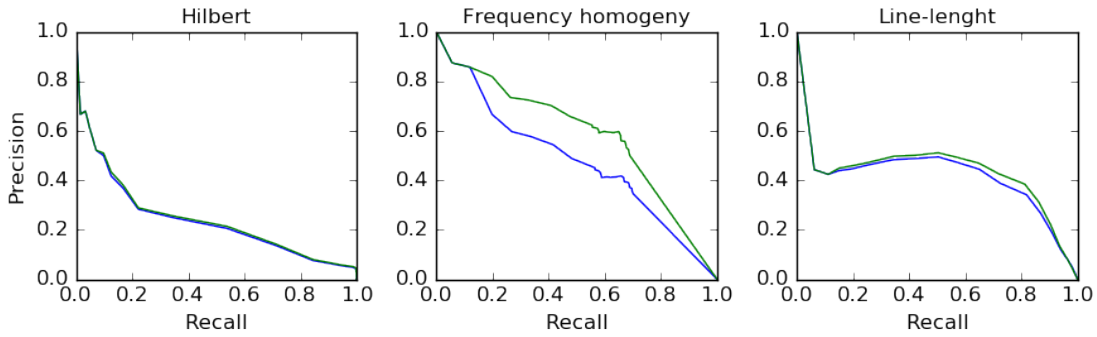

Figure 12: ***Precision-recall analysis of gold standard HFO detection.***

Precision-recall curves of agreement with gold standard reviewer marks. Blue – automated detection, green – semi-automated detection.

Algorithm	Mode	F^1	F^2	F^{05}
Hilbert	Automated	3.993	6.238	6.238
	Semi - Automated	3.991	6.236	6.236
Frequency homogeny	Automated	2.669	4.17	4.17
	Semi - Automated	2.599	4.061	4.061
Line-length	Automated	3.273	5.114	5.114
	Semi - Automated	3.248	5.074	5.074

Table 2: ***F-scores for gold standard evaluation.***

8.4.2 Results of feature estimation precision

The analysis of amplitude estimation precision revealed that all algorithms overestimated event amplitude (Figure 13, Table 3). Increased amplitude of simulated events showed improved mean amplitude estimation error in all detectors, however, the standard deviation increased. The best performing algorithm for this feature was the Hilbert detector while frequency homogeny and line-length detectors showed similar results.

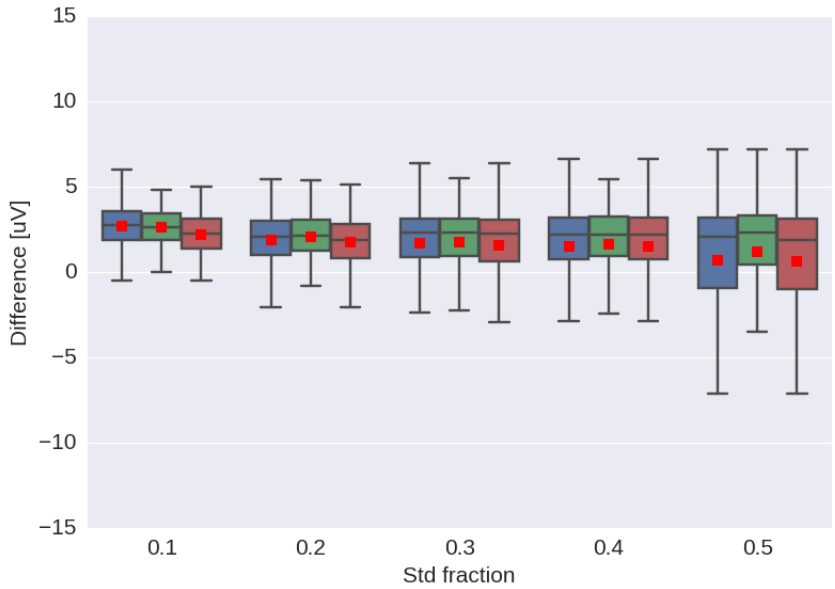

Figure 13: ***Amplitude estimation analysis.***

Higher event amplitude improves automated estimation but increases its standard deviation. Red square – mean value. Blue – line-length, green – frequency homogeny, red – Hilbert.

Similarly to amplitude, all algorithms exhibited overestimation of duration (Figure 14, Table 3). Changes in artificial event amplitude did not have any impact on duration estimation. The Hilbert algorithm was the best performing while the worst was line-length algorithm.

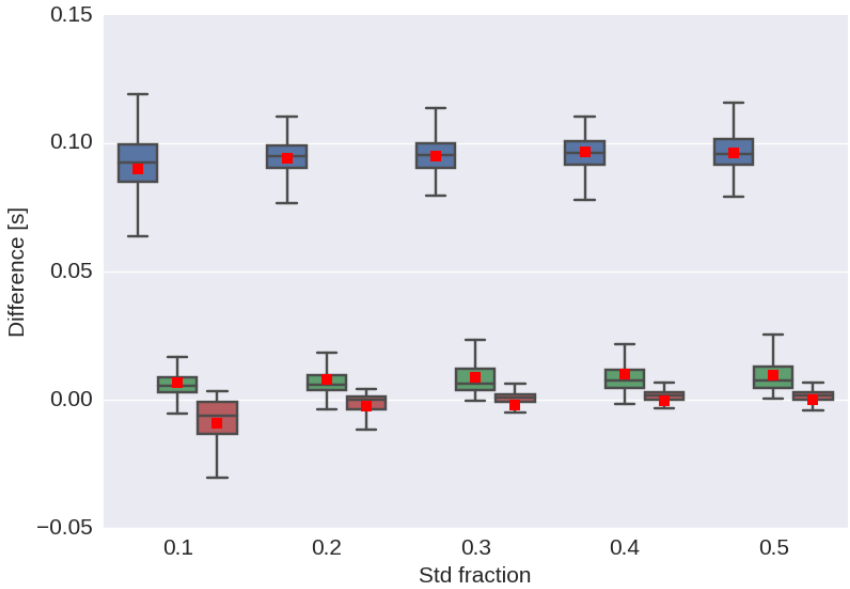

Figure 14: ***Duration estimation analysis.***

Higher event amplitude improves duration estimation in Hilbert algorithm. Frequency homogeny a line-length algorithms show stable estimation. Red square – mean value. Blue – line-length, green – frequency homogeny, red – Hilbert.

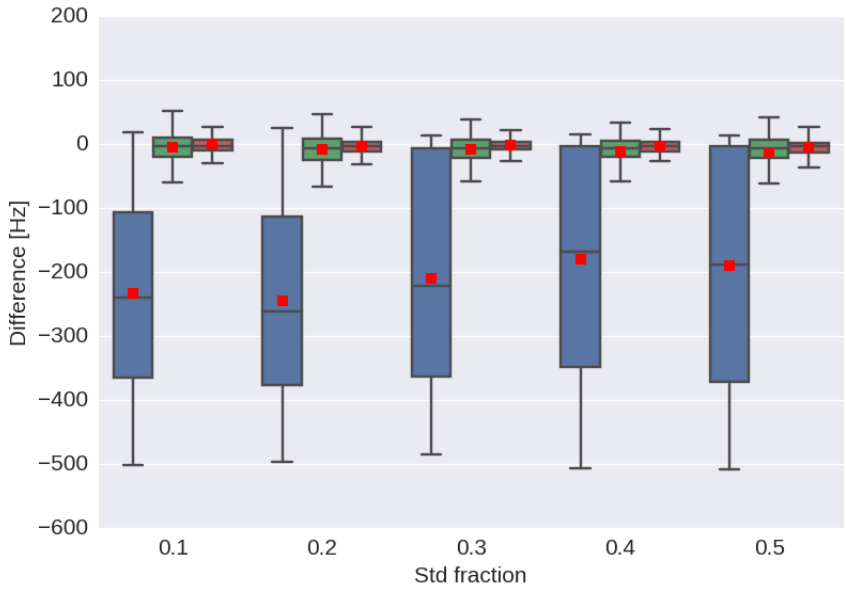

Figure 15: ***Frequency estimation analysis.***

Hilbert detection algorithm shows the lowest difference with referential values. Line-length algorithm exhibits the highest error. Red square – mean value. Blue – line-length, green – frequency homogeny, red – Hilbert.

Contrary to amplitude and duration all algorithms underestimated frequency irrespective of the event amplitude (Figure 15, Table 3). Increasing event amplitude worsened frequency estimation in Hilbert detector and frequency homogeny detector only in transition between the lowest threshold setting to the second lowest setting. The most precise algorithm was the Hilbert algorithm and the worst was the line-length algorithm.

In general, Hilbert algorithm showed best performance in analysis of feature estimation. Frequency homogeny algorithm performed roughly similarly to line-length detector in amplitude estimation but was worse in duration and frequency estimation. Line-length algorithm had poorest performance in feature estimation. Noise in signal had the highest impact on amplitude estimation. Duration and frequency showed similar mean differences as the signal without noise (Table 3, Table 4).

		STD fraction				
Feature	Algorithm	0.1	0.2	0.3	0.4	0.5
Amplitude	FH	2.033	1.488	1.751	1.755	0.761
	Hilbert	1.704	1.213	1.371	1.415	0.632
	LL	2.366	1.564	1.717	1.609	0.664
Duration	FH	0.009	0.011	0.011	0.012	0.011
	Hilbert	-0.001	0.001	0.002	0.003	0.002
	LL	0.095	0.096	0.104	0.097	0.095
Frequency	FH	-6.526	-11.126	-14.242	-10.71	-17.863
	Hilbert	-0.091	-8.234	-6.193	-4.917	-6.342
	LL	-212.206	-189.411	-148.561	-92.388	-93.625

Table 3: ***Mean feature differences from artificial HFO events – clean signal.***

		STD fraction				
Feature	Algorithm	0.1	0.2	0.3	0.4	0.5
Amplitude	FH	2.614	2.077	1.766	1.645	1.157
	Hilbert	2.197	1.739	1.584	1.515	0.647
	LL	2.701	1.900	1.672	1.518	0.713
Duration	FH	0.007	0.008	0.009	0.010	0.010
	Hilbert	-0.009	-0.002	-0.002	0.000	0.000
	LL	0.090	0.094	0.095	0.097	0.096
Frequency	FH	-4.741	-7.901	-8.588	-12.069	-13.648
	Hilbert	-0.706	-3.273	-2.492	-3.629	-4.542
	LL	-232.771	-245.602	-210.731	-180.773	-189.701

Table 4: **Mean feature differences from artificial HFO events - noisy signal.**

8.4.3 Results of pathologic tissue localization

Investigation of pathological tissue localization with regard to detector threshold revealed a trend for line-length detector where higher thresholds improved localization both in normal vs. pathological (SOZ + IZ), normal vs. SOZ analysis (disregarding IZ) and resected channels in patients with good outcomes (Table 5).

Threshold analysis of pathological tissue localization revealed that line-length and Hilbert algorithms showed a similar trend where increasing threshold led to improved detection. Contrary to the other two algorithms frequency homogeny detector had inverse trend where the lowest threshold achieved the best results. The best performing thresholds were 5, 0.1, 5 for line-length, frequency homogeny and Hilbert algorithms respectively.

ROC curves for best performing thresholds were done for pathology, SOZ and resected channels as target instances (Table 5 and Figure 16). Line-length detector had the highest values of AUC for pathology and SOZ analysis. Hilbert detector had the highest AUC for resected channels.

Using per patient normalized HFO rates generally improved performance of all HFO detectors.

Algorithm	Feature	Pathology	Seizure onset zone	Resection
Line-length	HFO count	0.778	0.951	0.704
	normalized HFO count	0.783	0.957	0.709
Hilbert	HFO count	0.537	0.787	0.719
	normalized HFO count	0.613	0.822	0.803
Frequency homogeny	HFO count	0.565	0.628	0.637
	normalized HFO count	0.593	0.584	0.752

Table 5: ***AUC values for pathological channel localization of different algorithms.***

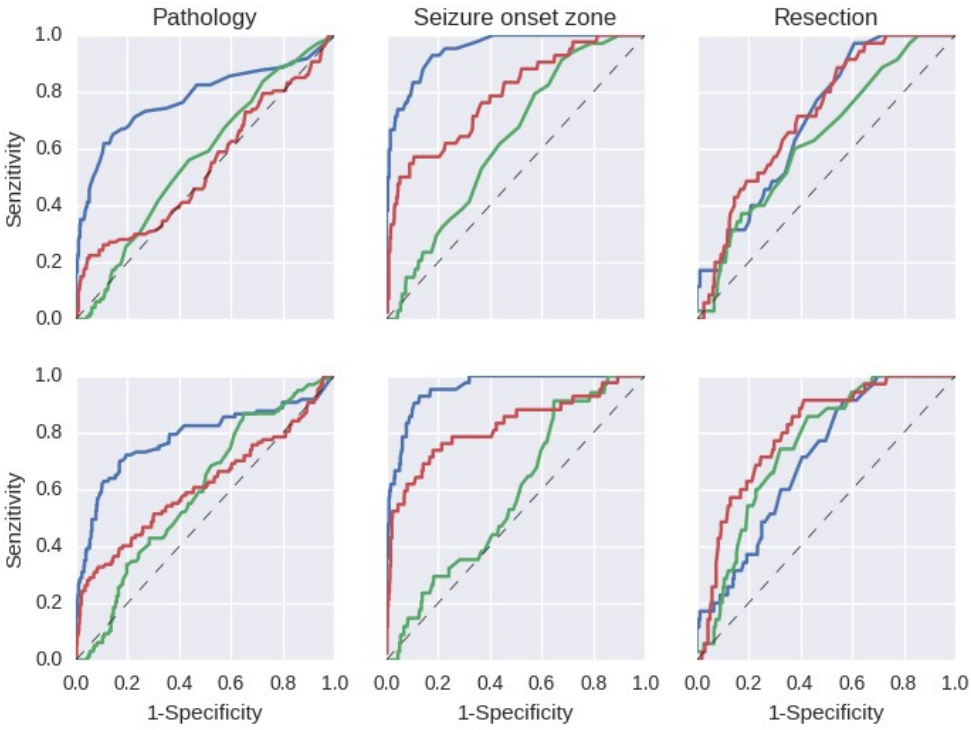

Figure 16: ***ROC analysis of pathologic tissue localization.***

ROC curves for localization of pathological tissue. Line-length algorithm outperforms the other two in clinically determined channels (Pathology, Seizure onset zone) but is the worst in determination of resected channels in patients with good outcome. Hilbert algorithm shows the best performance in this regard. Top – ROC for HFO rates, bottom – ROC for per patient normalized HFO rates. Blue – line-length, green – frequency homogeny, red – Hilbert.

8.4.4 Algorithm speed results

The fastest algorithm was the line-length based detector which processed the dataset in 265 s which is 6.79 times faster than real time (30 mins). The second algorithm was the frequency homogeny with the computation time of 1592 s which is 1.13 times faster than real time. The slowest algorithm was the Hilbert detector with the processing time of 7840 s and 0.23 times slower than real time.

8.5 Summary of results and discussion

Four types of evaluation were performed: ability of detectors to correctly detect gold standard HFOs marked by expert reviewers, ability to correctly estimate HFO features, ability to correctly localize tissue that exhibits pathologic electrophysiologic activity (SOZ+IZ), seizure onset zone (SOZ) or resected channels in patients with good surgical outcome and processing time of each algorithm.

Evaluation of detector performance based on expertly reviewed events is often used in scientific literature dealing with HFO detection [61, 63, 64]. Even though this method is generally accepted there are certain drawbacks already discussed in the chapter 8.2.1. Within the scope of this work the best performing algorithm was the one based on the frequency homogeny metric. This result confirms the assumption that the algorithm improves specificity compared to earlier and simpler detectors such as line-length and RMS detector [41, 51]. Higher specificity can be explained by the novel metric which effectively eliminates Gibb's phenomenon as well as to post-processing steps that take reviewer expertise into account.

The second best performing algorithm was the line-length algorithm with added simple post-processing steps. The results in this work corroborate previous findings in earlier studies [51, 64]. The fact that the specificity is lower might reflect insufficient elimination of Gibb's phenomenon with use of correlation and detection of events that are not visible for naked human eye.

The design and purpose of the algorithm based on Hilbert envelopes, which is feature extraction while maintaining high sensitivity, was reflected in very poor specificity. This confirms that post-processing steps or methods of machine learning have to be applied in order to achieve better concordance with human reviewers.

Results of the same analysis performed in semi-automated fashion where noisy segments were removed by reviewers improved in all tested algorithms. The highest improvement by 0.07 in F_1 score was seen in frequency homogeny algorithm. This suggest that either a manual or automated detection of noise and artifacts can lead to a substantial increase in performance.

Detection matching to reviewed events and HFO occurrence in individual channels is often the main focus of HFO detection algorithms. In some works, HFO features such as frequency and duration are described [23, 38], nonetheless the method by which these features were acquired is often not clearly stated. In papers dealing with HFO detection the performance of algorithms in feature estimation is usually completely disregarded.

This aspect of detectors was evaluated using artificial HFO events with known amplitude, frequency and duration that were inserted into one channel of non-pathologic iEEG signal. Increasing event amplitude was applied to estimate change in feature estimation error.

All algorithms showed trend to overestimate the amplitude. This could be ascribed to the noise of the original iEEG signal into which the artificial signals were inserted. Increased amplitude of simulated events showed improved mean amplitude estimation in all detectors which is likely due to higher signal to noise ratio but the standard deviation of the estimation error increased presumably because of high amplitude of spikes in HFO-spike artificial events. The Hilbert algorithm showed the best performance which is likely due to precise detection of event onset and offset.

Analysis of duration estimation precision revealed the same trend as with amplitude where all algorithms overestimated this feature. This could be caused by algorithm methodology, which is further discussed below, and by filtration that smears the extent of the event to some extent. The worst performing algorithm was the line-length based algorithm while the Hilbert algorithm showed the best performance. These results stem from the algorithm nature since line-length algorithm utilizes sliding window with only 25 % overlap it introduces error into duration estimation. Contrarily, Hilbert algorithm uses sample by sample detection leading to higher precision. Frequency homogeny algorithm introduces estimation error likely due to the sliding window nature of frequency homogeny metric.

Frequency estimation showed inverse trend to those of duration and amplitude and all algorithms underestimated frequencies of simulated events which could be ascribed to frequency band sequences used by these detectors. Hilbert detector and frequency homogeny detector showed stable frequency estimation with increasing event

amplitude which worsened only in transition between the lowest threshold setting to the second lowest setting. The possible cause here is the more precise detection of event onset and offset with lowest threshold settings. The frequency calculation in line-length algorithm is done in post-processing steps using the maximum peak in frequency spectrum leading to a substantial error which, however, diminishes with increasing event amplitude where the maximum spectrum peak is more prominent.

In summary, the Hilbert detector outperformed the other two detectors in estimation of all evaluated features. This result confirms that the Hilbert detector design is the most suitable tool for in depth study of HFOs. Frequency homogeny algorithm performance exhibited reasonable estimation error proving that it can be used for rough overview of HFO features in the detected dataset. Line-length detector showed the poorest performance which is due to the simplistic nature of the algorithm.

The capability of pathological tissue localization is vital for clinical applications. This is often tested in the literature along with analysis of successful detection of gold standard detections [54, 62, 63]. While this approach is the most important in clinical applications the best performance in this regard does not necessarily mean that the algorithm can as efficiently serve for basic research of HFO.

All algorithms were able to successfully show increased HFO activity in pathological tissue based on HFO detection. Relatively high thresholds in line-length and Hilbert detector showed the best performance with regard to SOZ localization. This can be explained by the core of these algorithms which is based mainly on signal amplitude. Frequency homogeny algorithm showed the best performance in the lowest threshold setting.

Analysis of tissue generating pathological interictal epileptiform spikes and HFOs (SOZ+IZ) decreased the performance of all algorithms. HFOs have been proved to be more localized in SOZ [25], thus this finding corroborates these previous results.

Analysis of HFO rates in patients with good surgical outcome showed improvement in frequency homogeny and Hilbert algorithm while decreasing the performance of line-length algorithm. The result highlights low specificity of line-length algorithm suggesting that it might be influenced by false positive detections of spikes.

ROC curves were created with the best performing threshold of each algorithm with HFO rate in individual channels as the threshold metric and pathological channels as targets. Interestingly, the line-length algorithm showed the best performance in SOZ localization while frequency homogeny the worst. Hilbert algorithm showed the best localization of resected channels. When the HFO rates were normalized on the per patient bases the results improved for resected channels in patients with good outcome suggesting that HFO rates may vary depending on implantation sites and patient's brain.

Processing time for each algorithm was measured using one iEEG signal. Line-length algorithm had the shortest processing time mainly due to its simplicity. Frequency homogeny algorithm needed more processing time but it was still faster than real time. Hilbert detection algorithm was approximately 5 times slower than real time suggesting that a compiled version of the algorithm should be developed in order to allow this algorithm to be used in clinic.

The line-length algorithm with simple post-processing steps (correlation and event to background ratio) showed very poor feature estimation yet the localization of SOZ was superior to other detectors. However, in localization of resected channels the algorithm performed poorly. With its speed this algorithm can be very useful in online HFO detection and use in clinic to give clinicians a rough idea about the HFO distribution in epileptic foci, thus highlighting the channels they should focus on.

Feature estimation error was the lowest for the Hilbert algorithm. This outcome demonstrates the algorithm's capability of HFO feature precise determination. Given the results in analysis of gold standard HFOs and pathologic tissue localization analysis this algorithm shows promising results that can be further improved by post-processing steps and machine learning methods.

Frequency homogeny algorithm showed the best performance in concordance with gold standard detections. Interestingly, the analysis of SOZ channel localization did not reveal good results but localization of resected channels was superior to line-length while inferior to Hilbert algorithm. As mentioned earlier in this work HFO marking is highly subjective. Enlarging the dataset on which the algorithm was trained is likely to improve the results. Feature estimation evaluation revealed that this detector can provide rough estimation of detected events' features.

9 DETECTION RESULT PRESENTATION

Conveying the results in simple and visually appealing way to the interpreter while preserving as much information as possible is crucial for wide spread usage of any detection algorithm in clinic and science. Medical doctors and some scientists often lack the technical skills and time to understand the details of signal processing and automated detection. Consequently, development of result presentation is almost as important as the detection itself.

In this regard information acquired from the brain present a challenge. The electrophysiological signals have intrinsic features – amplitude and frequency. In case of HFOs, two other features can be acquired – duration and count. However, the physiology of the brain and its electrical properties change in time (cognition, sleep, etc.), space (neocortex, archicortex, etc.) and is dependent on external factors (drugs, external stimuli, etc.).

As it is apparent from the previous paragraph, it is not possible to visualize all information at once. Instead, the visualizations are focused on the desired application. Nonetheless, the interpreter should always be aware of the limitations.

9.1 HFO count per channel

Basic visualization used by vast majority of current publications dealing with HFO is usually a simple bar graph used to highlight channels with higher HFO occurrence (Figure 17). While this is sufficient for a general overview the loss of information about HFOs is significant. There is no information about HFO occurrence in time domain, which obstructs a potential feedback by medical staff or adjustment of medication. The frequency information is reduced to that of the frequency band used by algorithm filters. And the person reading the plot has to be aware of the individual contact locations within the brain in order to interpret the results correctly.

This type of visualization could stress the results by color-coding the HFO count in individual bars which would make it easier to identify the channels of interest.

Furthermore, temporal information could be included by creating a video or by plotting numerous bar graphs for each time segment.

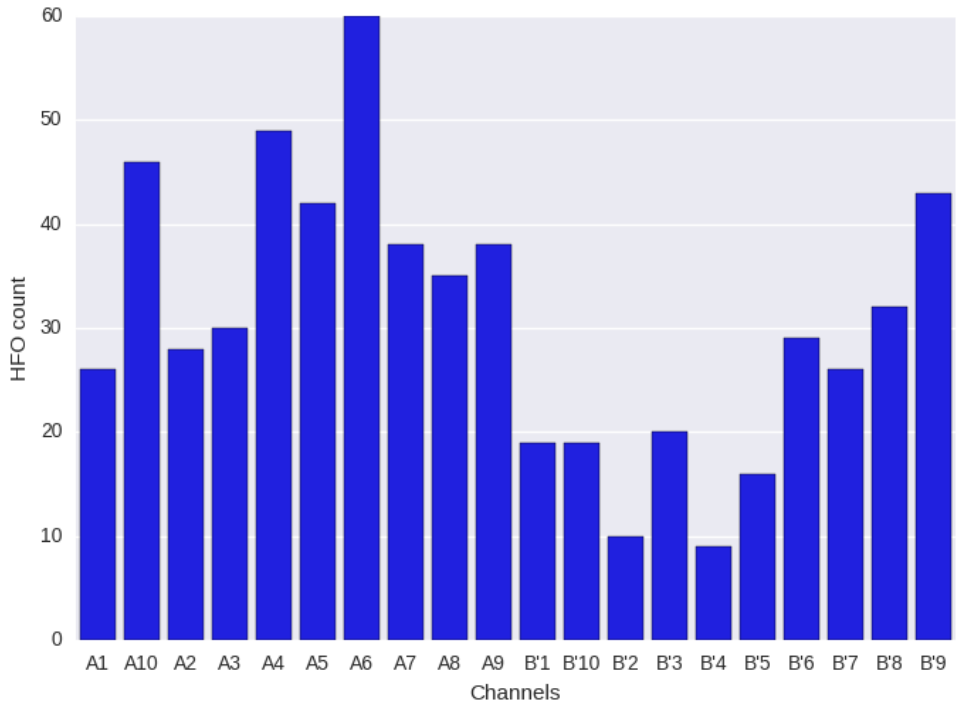

Figure 17: ***Bar graph of HFO counts in individual channels.***

Bar graph showing the count of detected HFOs in individual channels. Without the knowledge of contact location in patient's brain it is difficult to determine the epileptogenic foci. Moreover, there is no information about the frequency of HFOs.

9.2 HFO count with regard to HFO frequency

This type of visualization was created as part of this PhD thesis and is useful for clinicians since fast ripples (250 – 600 Hz) are currently deemed to be correlated with pathologic brain more than ripples (80-250 Hz). The color-coded table presents HFO counts in individual frequencies and provide simplified information about the HFO distribution in frequency domain. The visualization was designed to present results of frequency homogeny algorithm, hence the frequency bands are set accordingly.

Even though, this visualization provides fast overview about the tissue surrounding individual contacts there is still some information loss. Temporal aspect of HFO occurrence is completely neglected and information about HFO are represented solely by their count in frequency bands.

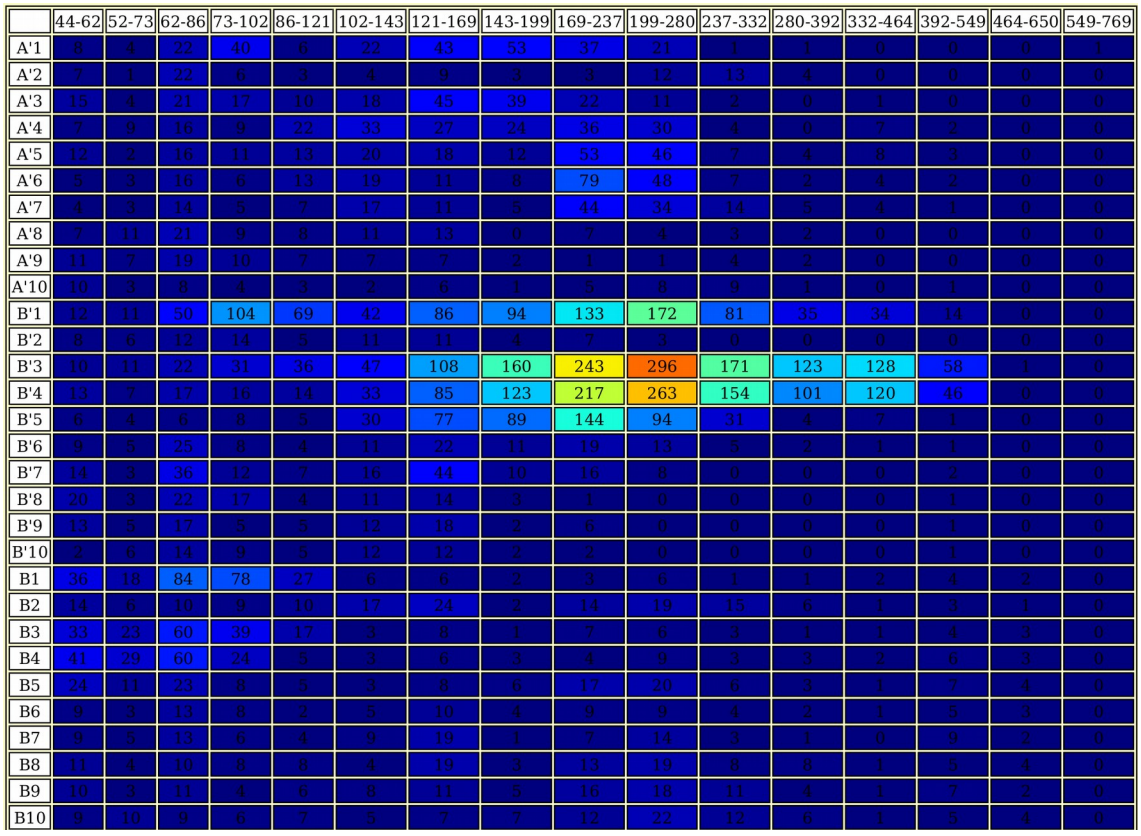

	44-62	52-73	62-86	73-102	86-121	102-143	121-169	143-199	169-237	199-280	237-332	280-392	332-464	392-549	464-650	549-769
A'1	8	4	22	40	6	22	43	53	37	21	1	1	0	0	0	1
A'2	7	1	22	6	3	4	9	3	3	12	13	4	0	0	0	0
A'3	15	4	21	17	10	18	45	39	22	11	2	0	1	0	0	0
A'4	7	9	16	9	22	33	27	24	36	30	4	0	7	2	0	0
A'5	12	2	16	11	13	20	18	12	53	46	7	4	8	3	0	0
A'6	5	3	16	6	13	19	11	8	79	48	7	2	4	2	0	0
A'7	4	3	14	5	7	17	11	5	44	34	14	5	4	1	0	0
A'8	7	11	21	9	8	11	13	0	7	4	3	2	0	0	0	0
A'9	11	7	19	10	7	7	7	2	1	1	4	2	0	0	0	0
A'10	10	3	8	4	3	2	6	1	5	8	9	1	0	1	0	0
B'1	12	11	50	104	69	42	86	94	133	172	81	35	34	14	0	0
B'2	8	6	12	14	5	11	11	4	7	3	0	0	0	0	0	0
B'3	10	11	22	31	36	47	108	160	243	296	171	123	128	58	1	0
B'4	13	7	17	16	14	33	85	123	217	263	154	101	120	46	0	0
B'5	6	4	6	8	5	30	77	89	144	94	31	4	7	1	0	0
B'6	9	5	25	8	4	11	22	11	19	13	5	2	1	1	0	0
B'7	14	3	36	12	7	16	44	10	16	8	0	0	0	2	0	0
B'8	20	3	22	17	4	11	14	3	1	0	0	0	0	1	0	0
B'9	13	5	17	5	5	12	18	2	6	0	0	0	0	1	0	0
B'10	2	6	14	9	5	12	12	2	2	0	0	0	0	1	0	0
B1	36	18	84	78	27	6	6	2	3	6	1	1	2	4	2	0
B2	14	6	10	9	10	17	24	2	14	19	15	6	1	3	1	0
B3	33	23	60	39	17	3	8	1	7	6	3	1	1	4	3	0
B4	41	29	60	24	5	3	6	3	4	9	3	3	2	6	3	0
B5	24	11	23	8	5	3	8	6	17	20	6	3	1	7	4	0
B6	9	3	13	8	2	5	10	4	9	9	4	2	1	5	3	0
B7	9	5	13	6	4	9	19	1	7	14	3	1	0	9	2	0
B8	11	4	10	8	8	4	19	3	13	19	8	8	1	5	4	0
B9	10	3	11	4	6	8	11	5	16	18	11	4	1	7	2	0
B10	9	10	9	6	7	5	7	7	12	22	12	6	1	5	4	0

Figure 18: ***Color-coded HFO rate in individual electrodes across frequencies.***

Image showing HFO occurrence in individual channels and in frequency bands with color-coded cells to stress the highest values. Color-coding contributes to simple immediate recognition of the areas with highest HFO rates.

This type of visualization can be further developed by creating a video where changing colors would show shifts in HFO counts with regard to channels and frequency. This would account for temporal changes.

9.3 HFO count with regard to anatomy

Anatomical structure may play a crucial role in spatial distribution of HFO. It is, therefore, useful to visualize the information about HFO occurrence in MRI scans so that clinical staff has immediate information about the location of HFO generating tissue and can tie together the information of electrophysiology and anatomy of the particular patient's brain.

This method was created as a diploma thesis [66] which was mentored by the author of this work.

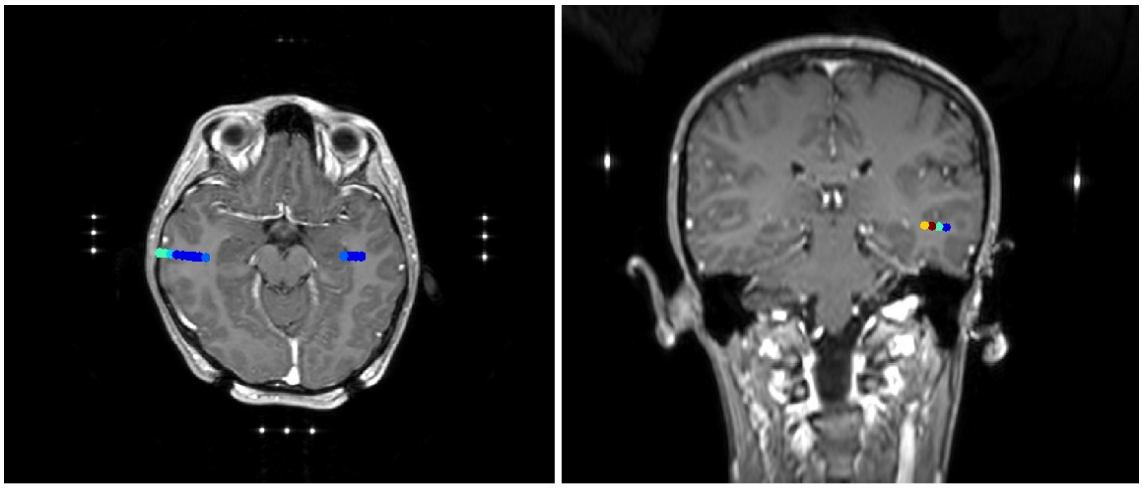

Figure 19: ***Color-coded HFO count in MRI slices.***

MRI scan of a patient with temporal lobe epilepsy. HFO counts are color coded as dots in places where electrode contacts were located. A – transversal plane B- coronal plane.

Further enhancements of this type of visualization can be again incorporation of information about HFO occurrence in time by creating video clips. Moreover, tractography analysis can be joined with this visualization in order to elucidate communication between different brain structures.

9.4 Circular graphs

Inspired by data visualization in genome research, this type of graph reduces information loss to minimum while allowing for display of interactions between areas of the brain from which iEEG signal is acquired. The visualization was created within this work and is freely available as an open-source library which is being actively updated and developed (https://github.com/cimbi/pancircs) and can be easily installed through python package index.

Circular graphs can have multiple layers each expressing different piece of information. HFO counts and their mean attributes can be simply visualized this way although any type of electrophysiological information can be included such as spike rates or their features. Individual layers can also represent development of HFO occurrence in time, space and frequency.

Inner area of the circular graph can be used to visualize interactions between signals such as correlation or other connectivity metrics which can contribute to correct localization of pathologic tissue.

Channels can be grouped according to their location in brain structures but any grouping variable can be used.

Circles can be assembled into a series to create either an array or a video to capture the development of electrophysiological data in time.

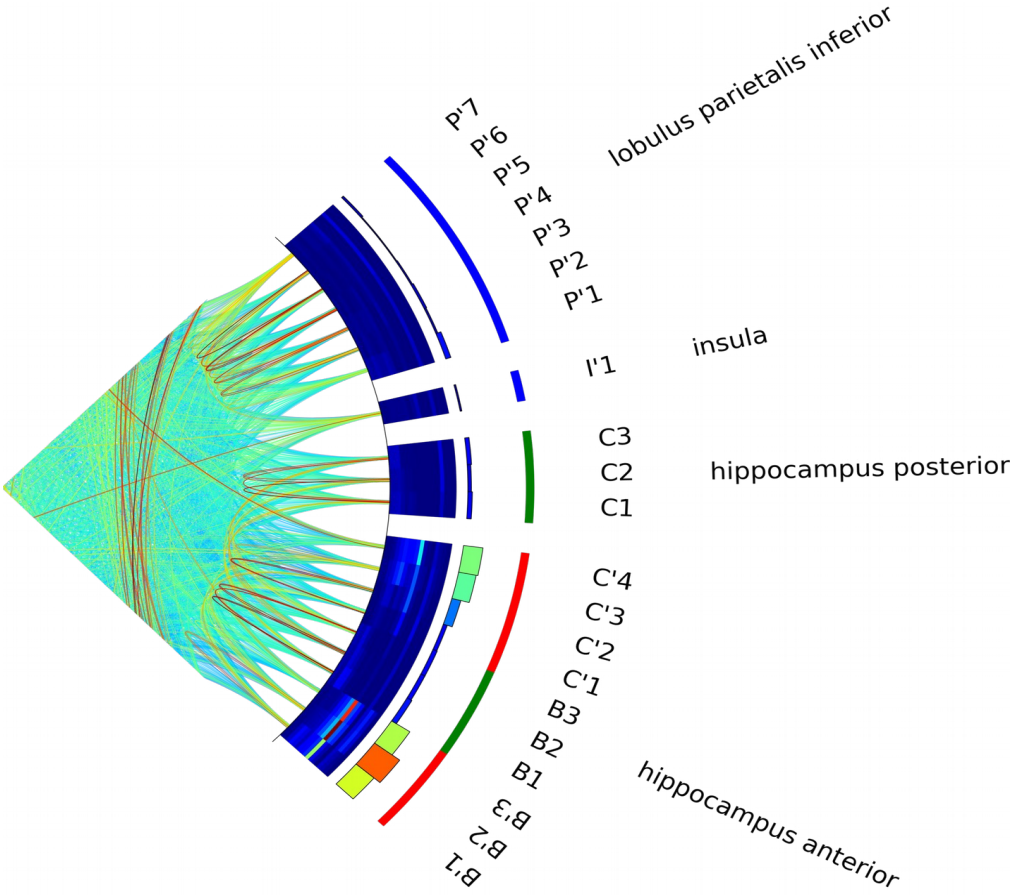

Figure 20: ***Circular visualization.***

Correlation between individual contacts (inner connections). Histogram of HFO count in frequency bands from low frequencies to high, inner to outer direction (inner circle). Total relative HFO count (middle circle). Pathology of channels (outer circle, SOZ -red, IZ – green, nonSOZ – blue). Contact sections are divided according to the structure in which they were located

10 ACHIEVED SCIENTIFIC RESULTS

Even though all described algorithms are constantly being improved they have already been used for clinical and research applications both at Mayo Clinic as well as FNUSA. This section is a brief result summary of finished and ongoing studies that serves as a proof of concept.

10.1 Spatiotemporal dynamics of high-frequency oscillations

The aim of this study was to evaluate the feasibility of line-length detection algorithm, investigate the localization of SOZ by HFOs and map the spatiotemporal characteristics of HFO occurrence in different brain structures and in different behavioral states. The reference to this study can be found in [67].

10.1.1 Data

91 epileptic patients with focal epilepsy were implanted with clinical hybrid depth electrodes (micro-electrode + macro-electrode) as part of their evaluation for partial surgical medio-temporal lobectomy.

The data were continually acquired during patients' stay in the intensive care unit at the sampling frequency of 32 kHz. For storage purposes and reduction of computation time all macro electrode recordings were filtered by a low pass filter (cut-off 1 kHz) and decimated to 5 kHz. Because the HFOs were proved to be present in both macro and microelectrode recordings the detection algorithm was run only on macro electrode recordings to achieve better clinical relevance and further reduce computation time. No time segments were excluded from the study.

To determine the seizure onset zone, an automated seizure detector with very high sensitivity was run on all acquired data prior to human assessment. The detections were then visually reviewed by an experienced neurologist and the first clear visible change in iEEG leading to propagating seizure discharges were marked as the seizure onset and the corresponding channels were marked as seizure onset channels.

Two experienced neurologists used pre-operative MRI and post-operative CT images to manually co-register the contact locations for each patient. The MNI coordinates were used to automatically assign a brain structure to each contact. Since the study was conducted solely in patients with medi-temporal epilepsy the structures used for analysis were amygdala, hyppocampus, parahyppocampus and neocortex.

To assess the effect of behavioral states, especially the slow wave sleep, on the HFO rate 7 recordings were scored by experienced sleep technicians. The individual behavioral states were – Awake, Stage I, Stage II, Stage III, REM, Unknown.

10.1.2 Brief summary of results

The evaluation of HFO rates in SOZ and nonSOZ proved that HFOs localize clinically marked epileptogenic areas in the vast majority of the patients. To assess the population statistics, using HFO rate in one channel as an instance, the Wilcoxon rank sum test was used with a highly significant result $p<0.001$. To further evaluate the applicability of results for prospective studies a separate Wilcoxon rank sum test for each patient was performed as well as paired t-test for the whole data set. Furthermore, to investigate the relationship of HFO rates in different structures of temporal lobe the channels were divided according to their localization in brain (32 patients with marked anatomical structures) and evaluated with regard to SOZ and nonSOZ. The result is demonstrated in Figure 21.

To investigate the temporal distributions of HFO rates 7 patients who had sleep staging were computed and evaluated in different sleep stages. Example figure that demonstrates HFO temporal changes with regard to sleep stages in one patient can be found in the supplement section (Supplement 4).

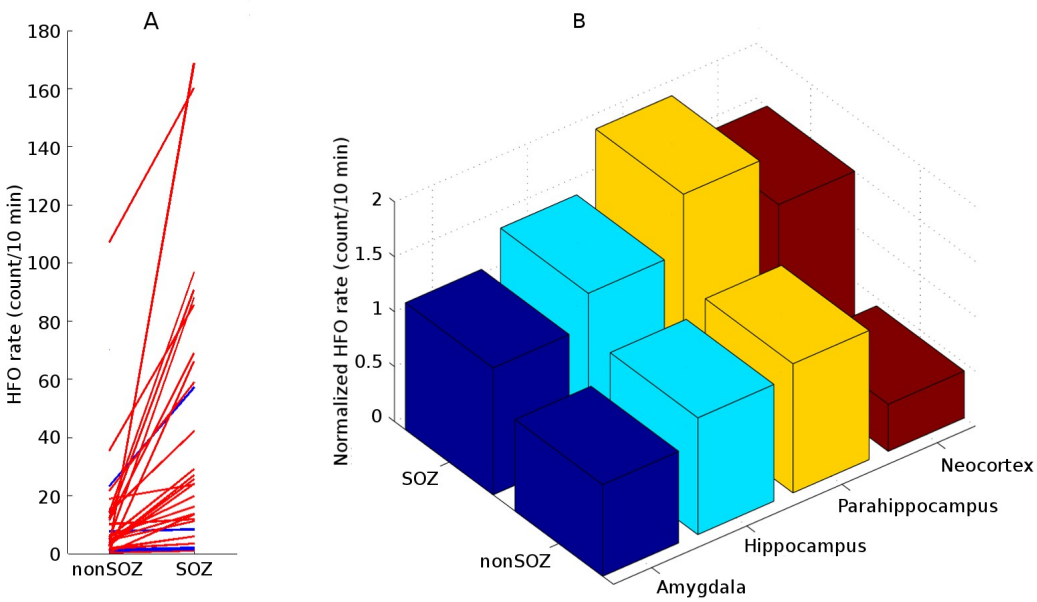

Figure 21: ***SOZ localization by HFO rate and spatial distribution of HFOs.***

(A) Mean HFO rates in SOZ channels and nonSOZ channels in a subset of 32 patients with focal temporal-lobe epilepsy. 28 patients (red ticks) had significantly higher HFO rate in contacts located in SOZ than in contacts located in nonSOZ area ($p<0.01$, Wilcoxon rank sum), 4 patients (blue ticks) did not show statistically significant level. (B) Normalized HFO rates in different areas of temporal lobe provides proof that pathological HFO rates in one structure might by similar to normal HFO rate in other structures.

10.2 High-frequency oscillations in cognitive processes

The study was conducted in order to investigate the relationship between HFOs and cognitive processing. The Hilbert 2D detector was used to detect HFOs during image presentations and their subsequent subjective evaluation in the brain. The whole study can be found in [68].

10.2.1 Data

Twelve patients undergoing intracranial seizure monitoring for surgical treatment participated in this voluntary study at Mayo Clinic. They were first presented a set of 80 images and were asked to rate the affective charge of each picture and remember it for subsequent recall 24h later. In every trial, image was displayed for 6s followed by 2s of blank screen. After that the patient was prompted to rate the picture's affective charge on a five-point scale, which ranged from 'very unpleasant' to 'very pleasant', by pressing a labeled key. The key press initiated an inter-trial interval of 6s preceding the next trial of this encoding stage of the task.

The recall stage of the task was analogous to the encoding, only this time 140 images were presented including the 80 pictures shown 24h earlier mixed with 60 new pictures. Images were presented for 6s, followed by 2s of blank screen and then a prompt screen asking the patient to indicate whether the image was 'old' or 'new' by pressing the labeled key. The key press triggered a second question asking the subject to rate their level of certainty on a five-point scale, which ranged from 'very certain' to 'very uncertain'. The key press initiated the 6s inter-trial interval preceding the next recall trial.

The acquired electrophysiological data were first decimated to 5000Hz, filtered between 0.1-1000Hz and notch-filtered to eliminate the 60Hz line noise. Bipolar differential signal was derived using recordings from neighboring pairs of electrodes to subtract out potential interference from the common reference, to ensure independence of the output signals in the analysis, and to reduce the non-cerebral artifacts. Data segments from the task encoding and recall stages were normalized by their standard deviation and cut into 18s epochs, which stretched from 6s preceding image

presentation to 6s following image disappearance. Every epoch was visually inspected for the occurrence of epileptiform discharges and artifacts, and rejected from the analysis if positive. Data from channels with more than 30 % of such epochs were not used in the study at all.

10.2.2 Brief summary of results

Changes of HFOs during cognitive processing associated with the encoding and retrieval of visual images was accompanied by focal increases of HFO power in all of the studied cortical and limbic structures. The pattern of power induction, confined to individual electrodes, was maintained across the HFO bands of high gamma, ripple and fast ripple frequencies. In contrast to the changes observed in the high frequency bands, theta/alpha/low beta oscillations (4-15Hz) showed widespread global reduction of power in response to image presentation (Figure 22).

HFOs recorded in different cortical and limbic structures of the processing stream revealed distinct pattern of gamma, ripple and fast ripple relative distributions. They lasted on average between 10-30ms and most those detected in the hippocampus and the amygdala had longer durations than the cortical discharges. Durations of the ripple band HFOs were consistently longer than the ones of the gamma and fast-ripple frequencies in all of the studied structures but the prefrontal cortex. Finally, the ripple and fast-ripple oscillations were very significantly modulated by the task phase (Figure 6) and predicted the affective value and memory of the images (Figure 23), suggesting an active role of these fast network events in cognitive processing.

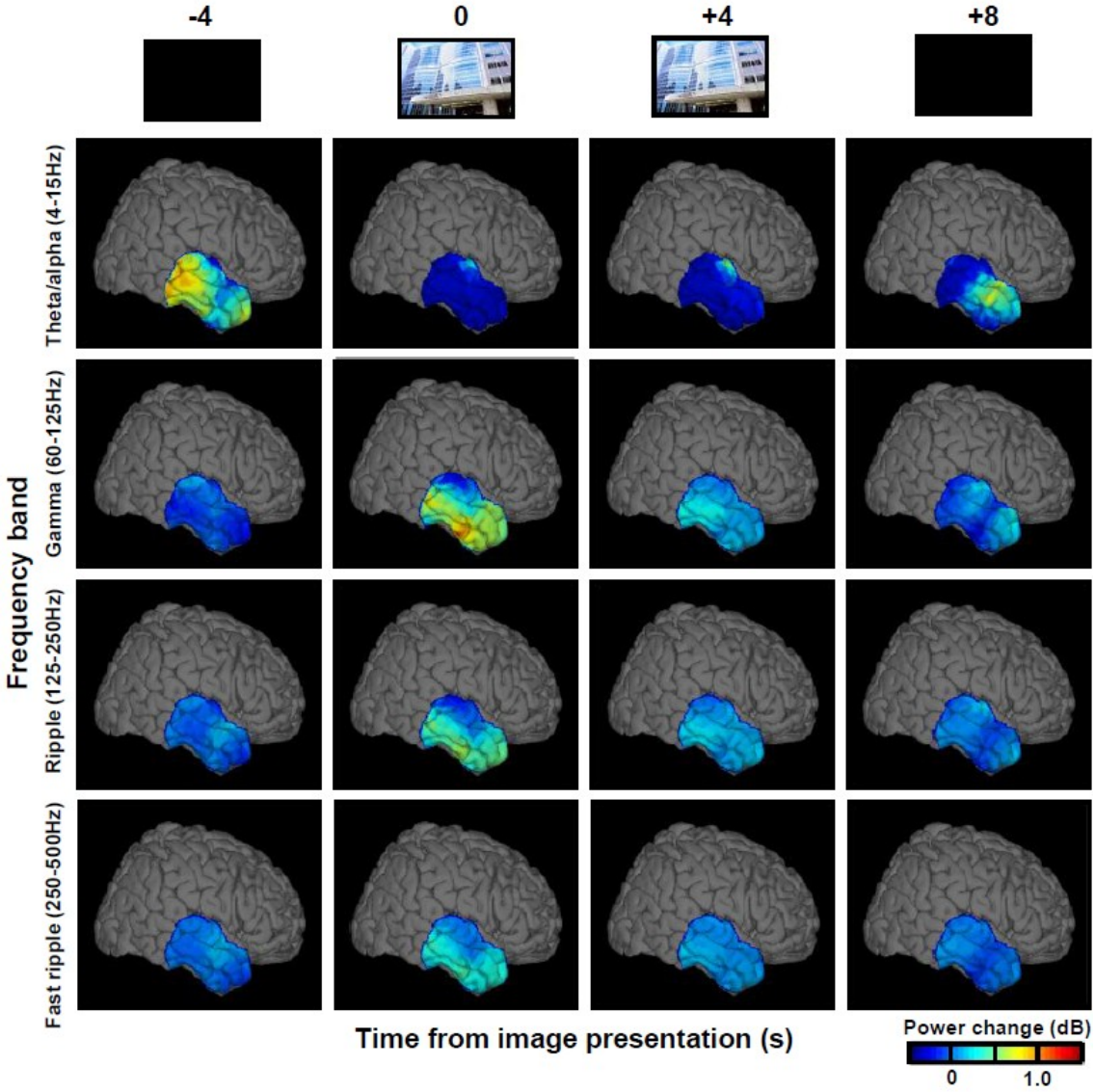

Figure 22: ***Frequency power during cognitive processes.***

Brain images of the normalized power changes recorded from temporal cortical surface grid electrodes in patient 8 are displayed for 4 frequency bands of oscillations, snapshot at 4 trial time-points of image encoding. Notice the focal pattern of activation in all HFO bands, including ripple and fast ripple frequencies, contrasted by uniform power decrease in the low frequencies.

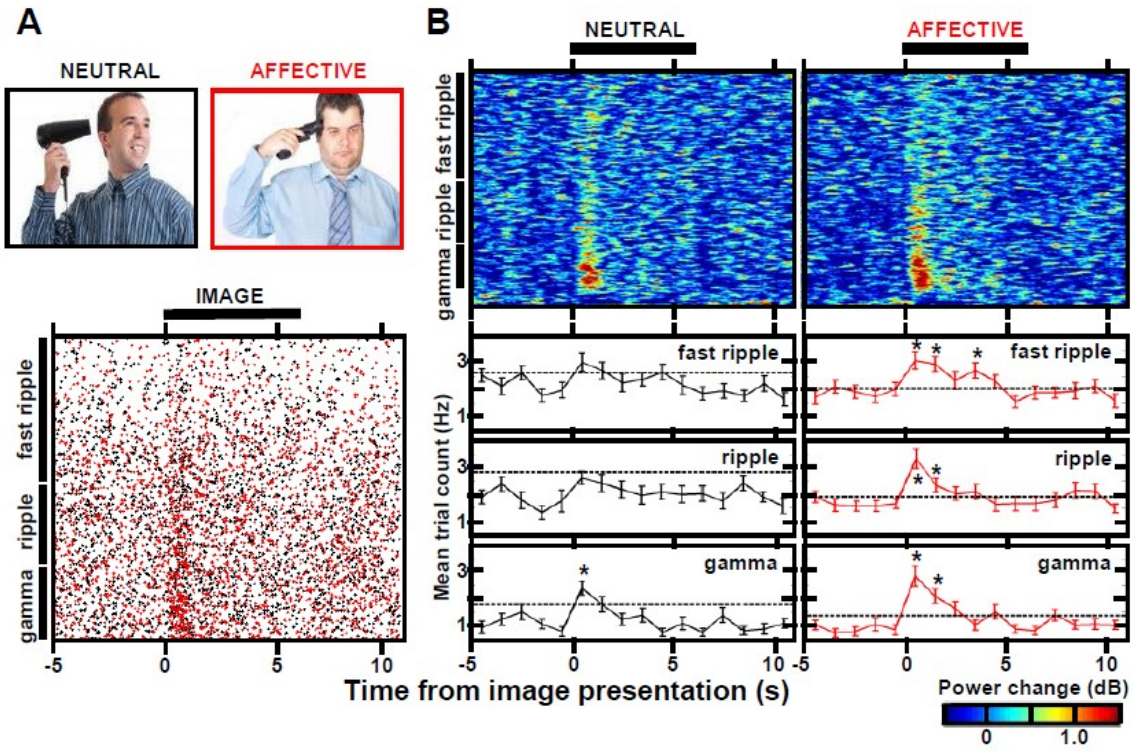

Figure 23: ***Local HFO band responses predict the affective value of encoded images.***

(A; top) Examples of two similar pictures, analogous to the IAPS set of images used in the study, with neutral and negative affective charge; (bottom) Cumulative scatterplot of the HFO discharges detected in the three frequency bands come from a representative amygdala electrode during the memory encoding (black dots are individual detections from trials with neutral images; red dots come from trials with emotionally charged images of the same session; black bar indicates time-course of image presentation). (B; top) Spectrograms summarize trial-averaged HFO band power changes in the two trial types from the same session as in 'A'; (bottom) mean trial counts of the gamma, ripple and fast ripple HFO detection from the same session are binned across the trial time-course aligned to the spectrograms (- $p<0.01$, Wilcoxon signed-rank test comparison with the matched average count from the 4 'baseline' bins preceding image presentation). Notice that this amygdala electrode shows enhanced HFO power underpinned by significantly increased number of HFO discharges on the trials with emotionally charged images.*

CONCLUSION

High-frequency oscillations have been studied for over a decade now. All the studies conducted to date have proven that HFOs can indeed localize epileptogenic foci in focal epileptic patients and that by resecting pathological tissue with HFO a better surgical outcome can be achieved, leading to improvement of patients' lives. Nonetheless, most of the studies used retrospective visual or semiautomated detections of HFOs. Such approach is a time-consuming process and is prone to reviewer bias. An automated detection algorithm is needed as a fast and objective method of detection.

A number of HFO detectors have been developed to date at different institutions around the world. However, due to unclear definition of HFOs, their characteristics and different recording techniques, all detectors were trained and tested on different datasets. Moreover, evaluation of developed detectors is not uniform rendering the results of automated HFO detection incomparable.

The main aim of the presented work was to develop a robust detector which would be useful for physicians and provide them with additional information about the localization and spatial spread of epileptogenic focus. The secondary goal was to create a tool for research of HFO produced by pathological and healthy tissue as well as during different cognitive stages such as somatosensory processing or sleep and wake cycle.

Three HFO detection algorithms were developed or enhanced in this work. One is the line-length algorithm which was improved by post-processing steps, aims at use in clinic and has already been used to investigate the spatiotemporal dynamics of HFOs in patients with mesio-temporal epilepsy. The second is an algorithm based on a novel frequency homogeny metric that effectively reduces the false positive detections and takes human expertise into account through a set of boundary thresholds calculated from distribution functions created from visually marked HFOs. The last algorithm was developed for detailed HFO analysis with precise HFO feature estimation and is based on normalized amplitude envelopes and convolution of narrow band-passed signal and broad-band passed signal. Its earlier version has been already used for study of HFO behavior during cognitive task to investigate the normal function of the brain.

To test the feasibility of detectors from different points of view all detectors were subjected to three different evaluation methods designed to overcome the common drawbacks appearing in literature. To test agreement with human reviewers the detections produced by automated methods were compared with gold standard detections created by manual review. Precision in HFO feature estimation was tested with artificial events inserted into iEEG signal and calculated feature values were compared with the known features of artificial events. Lastly, the ability to localize pathological tissue based on the count of HFO detections in individual channels was compared with clinically determined channels from which the seizures originated.

Results of evaluation confirmed effectiveness of each algorithm in the task they were designed for. While frequency homogeny algorithm had the best performance in agreement with gold standard detections, Hilbert algorithm showed the best feature estimation and localization of resected channels and line-length algorithm outperformed the remaining two in pathological tissue localization.

In order to convey the results to the end user, which is usually a clinician or a researcher, apt result visualization has to be chosen. Apart from wide-spread bar graph visualization of HFO count in individual channels, two other methods were developed in this work. One is a color-coded table with count in individual channels and frequency information. This allows clinicians to immediately evaluate the HFO analysis and is currently being used in St. Anne's University Hospital in Brno. The second method is inspired by visualization techniques in genome research and utilizes circular graphs. That allows for visualization of different HFO qualities as well as relationships between individual channels or brain structures.

The future work will focus on detector improvement and on combining their capabilities to provide better localization of pathological tissue while mapping the normal function of the brain. For that purpose more visually reviewed events will be acquired as well as data from multiple centers. HFO differentiation will be done with the use of machine learning methods and HFO spread will be studied with the use of brain connectivity methods and causality information. These future studies should improve both detection as well as general understanding of epilepsy and normal brain function.

All detection algorithms as well as evaluation codes mentioned in this work will be over time published online within the HFO-detect initiative (https://github.com/HFO-detect) that aims at creating a library of HFO detectors along with standardized evaluation tools. In conjunction with other algorithms developed around the world and publicly accessible iEEG datasets this will allow for objective evaluation of each algorithm with precisely defined evaluation methods. Moreover, it will allow other centers around the world that have not yet started using HFOs in their research and in clinic to immediately begin automated detection in intracranial EEG and contribute with their datasets to the world wide pool. Circular visualization library is already available for easy installation through python package index (name: “pancircs”) and the source code is accessible on GitHub (https://github.com/cimbi/pancircs).

REFERENCES

[1] HOLDEN, E Wayne, Hoang THANH NGUYEN, Elizabeth GROSSMAN, Scott ROBINSON, Leila S NELSON, Margaret J GUNTER, Ann VON WORLEY and David J THURMAN. Estimating prevalence, incidence, and disease-related mortality for patients with epilepsy in managed care organizations. *Epilepsia* [online]. 2005, vol. 46, no. 2, pp. 311–9. ISSN 0013-9580. Available at: doi:10.1111/j.0013-9580.2005.30604.x

[2] FISHER R, VAN EMDE BOAS W, BLUME W, ELGER C., GENTON P, LEE P, Engel J. Epileptic seizures and epilepsy: definitions proposed by the International League Against Epilepsy (ILAE) and the International Bureau for Epilepsy (IBE). *Epilepsia* [online]. 2005, vol. 46, no. 10, pp. 1698–9. ISSN 0013-9580. Available at: doi:10.1111/j.1528-1167.2005.00273_1.x

[3] RYAN, Monique M. *A Disease Once Sacred. A History of the Medical Understanding of Epilepsy* [online]. 2002. ISBN 0861966074. Available at: doi:10.1016/S0920-1211(02)00175-4

[4] MORÁŇ, Miroslav. *Praktická epileptologie*. 2003. ISBN 978-80-7387-023-2.

[5] C. P. PANAYIOTOPOULOS. *A clinical guide to epilepsy syndromes*. B.m.: Bladon medical publishing, 2010. ISBN 978-1-84628-644-5.

[6] CHRISTOPH, Helmstaedter. Neuropsychological aspects of epilepsy surgery. *Epilepsy & Behavior*. 2004, vol. 5, pp. 45–55.

[7] WORRELL, Gregory A, K JERBI, K KOBAYASHI, J. M LINA, Rina ZELMANN and M LE VAN QUYEN. Recording and analysis techniques for high-frequency oscillations. *Progress in neurobiology* [online]. 2012, vol. 98, no. 3, pp. 265–78 [accessed. 2013-10-26]. ISSN 1873-5118. Available at: doi:10.1016/j.pneurobio.2012.02.006

[8] AYALA, G F, M DICHTER, R J GUMNIT, H MATSUMOTO and W A SPENCER. Genesis of epileptic interictal spikes. New knowledge of cortical feedback systems suggests a neurophysiological explanation of brief paroxysms. *Brain research* [online]. 1973, vol. 52, pp. 1–17. ISSN 00068993. Available at: doi:10.1016/0006-8993(73)90647-1

[9] REN, L., Michal T. KUCEWICZ, Jan CIMBALNIK, Joseph Y MATSUMOTO, B. H. BRINKMANN, W. HU, W. R. MARSH, F. B. MEYER, S. M. STEAD and Gregory a WORRELL. Gamma oscillations precede interictal epileptiform spikes in the seizure onset zone. *Neurology* [online]. 2015, vol. 84, no. 6, pp. 602–608. ISSN 0028-3878. Available at: doi:10.1212/WNL.0000000000001234

[10] WORRELL, Gregory A and Jean GOTMAN. High-frequency oscillations and other electrophysiological biomarkers of epilepsy: clinical studies. *Biomarkers in medicine* [online]. 2011, vol. 5, no. 5, pp. 557–66. ISSN 1752-0371. Available at: doi:10.2217/bmm.11.74

[11] TELLEZ-ZENTENO, JF, LH RONQUILLO, F MOIEN-AFSHARI and S WIEBE. Surgical outcomes in lesional and non-lesional epilepsy: A systematic review and meta-analysis. *Epilepsy*. 2010, vol. 89, no. 2-9, pp. 310–318.

[12] MCBRIDE, MC, KS BRONSTEIN, B BENNETT, G ERBA, W PILCHER and MJ BERG. Failure of standard magnetic resonance imaging in patients with refractory temporal lobe epilepsy. *Archives of Neurology*. 1998, vol. 55, no. 3, pp. 346–348.

[13] WELLMER, J, CM QUESADA, L ROTHE, CE ELGER, CG BIEN and H URBACH. Proposal for a magnetic resonance imaging protocol for the detection of epileptogenic lesions at early outpatient stages. *Epilepsia*. 2013, vol. 54, no. 11, pp. 1977–1987.

[14] VAN BOGAERTA, P, N MASSAGERC, P TUGENDHAFTD, D WIKLERA, P DAMHAUTA, M LEVIVIERC, J BROTCHIC and S GOLDMANA. Statistical parametric mapping of regional glucose metabolism in mesial temporal lobe epilepsy. *Neuroimage*. 2000, vol. 12, no. 2, pp. 129–138.

[15] TAKAHASHI, M, T SOMA, K KAWAI, K KOYAMA, K OHTOMO and T MOMOSE. Voxel-based comparison of preoperative FDG-PET between mesial temporal lobe epilepsy patients with and without postoperative seizure-free outcomes. *Annals of nuclear medicine*. 2012, vol. 26, no. 9, pp. 698–706.

[16] JEONG TAE, Kim, Bai SUN JOON, Choi KEUM OK, Lee YOON JIN, Park HAE-JEONG, Kim DONG SEOK, Kim HEUNG DONG and Lee JOON SOO. Comparison of various imaging modalities in localization of epileptogenic lesion using epilepsy surgery outcome in pediatric patients. *Seizure - European Journal of Epilepsy*. 2009, vol. 18, no. 7, pp. 504–510.

[17] EINEVOLL, Gaute T, Christoph KAYSER, Nikos K LOGOTHETIS and Stefano PANZERI. Modelling and analysis of local field potentials for studying the function of cortical circuits. *Nature reviews. Neuroscience* [online]. 2013, vol. 14, no. 11, pp. 770–85 [accessed. 2015-12-20]. ISSN 1471-0048. Available at: doi:10.1038/nrn3599

[18] VAN DEN BROEK, S.P, F REINDERS, M DONDERWINKEL and M.J PETERS. Volume conduction effects in EEG and MEG. *Electroencephalography and Clinical Neurophysiology* [online]. 1998, vol. 106, no. 6, pp. 522–534. ISSN 00134694. Available at: doi:10.1016/S0013-4694(97)00147-8

[19] STEPHAN, Christina L., John J. KEPES, Karen SANTACRUZ, Steven B. WILKINSON, Barbara FEGLEY and Ivan OSORIO. Spectrum of Clinical and Histopathologic Responses to Intracranial Electrodes: From Multifocal Aseptic Meningitis to Multifocal Hypersensitivity-type Meningovasculitis. *Epilepsia* [online]. 2001, vol. 42, no. 7, pp. 895–901. ISSN 00139580. Available at: doi:10.1046/j.1528-1157.2001.042007895.x

[20] GORGULHO, Alessandra, Antonio a F DE SALLES, Leonardo FRIGHETTO and Eric BEHNKE. Incidence of hemorrhage associated with electrophysiological studies performed using macroelectrodes and microelectrodes in functional neurosurgery. *Journal of neurosurgery* [online]. 2005, vol. 102, no. 5, pp. 888–96. ISSN 0022-3085. Available at: doi:10.3171/jns.2005.102.5.0888

[21] STABA, Richard J, Charles L WILSON, Anatol BRAGIN, Donald JHUNG, Itzhak FRIED and Jerome ENGEL. High-frequency oscillations recorded in human medial temporal lobe during sleep. *Annals of neurology* [online]. 2004, vol. 56, no. 1, pp. 108–15 [accessed. 2014-01-29]. ISSN 0364-5134. Available at: doi:10.1002/ana.20164

[22] BRÁZDIL, Milan, Jan CIMBALNIK, Robert ROMAN, Daniel J SHAW, Matt M STEAD, Pavel DANIEL, Pavel JURÁK and Josef HALÁMEK. Impact of cognitive stimulation on ripples within human epileptic and non-epileptic hippocampus. *BMC Neuroscience* [online]. 2015, pp. 1–9. ISSN 1471-2202. Available at: doi:10.1186/s12868-015-0184-0

[23] BUZSÁKI, György, Z HORVÁTH, R URIOSTE, J HETKE and K WISE. High-frequency network oscillation in the hippocampus. *Science (New York, N.Y.)* [online]. 1992, vol. 256, no. 5059, pp. 1025–7. ISSN 0036-8075. Available at: http://www.ncbi.nlm.nih.gov/pubmed/1589772

[24] JACOBS, Julia, Pierre LEVAN, Rahul CHANDER, Jeffery HALL, François DUBEAU and Jean GOTMAN. Interictal high-frequency oscillations (80-500 Hz) are an indicator of seizure onset areas independent of spikes in the human epileptic brain. *Epilepsia* [online]. 2008, vol. 49, no. 11, pp. 1893–907 [accessed. 2014-01-09]. ISSN 1528-1167. Available at: doi:10.1111/j.1528-1167.2008.01656.x

[25] BRAGIN, Anatol, Jerome ENGEL, Charles L WILSON, Itzhak FRIED and Gary W. MATHERN. Hippocampal and entorhinal cortex high-frequency oscillations (100--500 Hz) in human epileptic brain and in kainic acid--treated rats with chronic seizures. *Epilepsia* [online]. 1999, vol. 40, no. 2, pp. 127–37 [accessed. 2013-10-28]. ISSN 0013-9580. Available at: doi:10.1111/j.1528-1157.1999.tb02065.x

[26] URRESTARAZU, Elena, Jeffrey D JIRSCH, Pierre LEVAN, Jeffery HALL, Massimo AVOLI, Francois DUBEAU and Jean GOTMAN. High-frequency intracerebral EEG activity (100-500 Hz) following interictal spikes. *Epilepsia* [online]. 2006, vol. 47, no. 9, pp. 1465–76 [accessed. 2014-01-20]. ISSN 0013-9580. Available at: doi:10.1111/j.1528-1167.2006.00618.x

[27] STABA, Richard J and Anatol BRAGIN. High-frequency oscillations and other electrophysiological biomarkers of epilepsy : underlying mechanisms. *Biomark Med.* [online]. 2011, vol. 5, no. 5, pp. 545–556. Available at: doi:10.2217/bmm.11.72.High-frequency

[28] IBARZ, Jose M, Guglielmo FOFFANI, Elena CID, Marion INOSTROZA and Liset MENENDEZ DE LA PRIDA. Emergent dynamics of fast ripples in the epileptic hippocampus. *The Journal of neuroscience : the official journal of the Society for Neuroscience* [online]. 2010, vol. 30, no. 48, pp. 16249–61 [accessed. 2013-11-08]. ISSN 1529-2401. Available at: doi:10.1523/JNEUROSCI.3357-10.2010

[29] USUI, Naotaka, Kiyohito TERADA, Koichi BABA, Kazumi MATSUDA, Fumihiro NAKAMURA, Keiko USUI, Takayasu TOTTORI, Shuichi UMEOKA, Shigeru FUJITANI, Tadahiro MIHARA and Yushi INOUE. Very high frequency oscillations (over 1000 Hz) in human epilepsy. *Clinical Neurophysiology* [online]. 2010, vol. 121, no. 11, pp. 1825–1831 [accessed. 2013-10-18]. ISSN 1872-8952. Available at: doi:10.1016/j.clinph.2010.04.018

[30] JERBI, Karim, Tomás OSSANDÓN, Carlos M HAMAMÉ, S SENOVA, Sarang S DALAL, Julien JUNG, Lorella MINOTTI, Olivier BERTRAND, Alain BERTHOZ, Philippe KAHANE and Jean-Philippe LACHAUX. Task-related gamma-band dynamics from an intracerebral perspective: review and implications for surface EEG and MEG. *Human brain mapping* [online]. 2009, vol. 30, pp. 1758–1771. ISSN 1097-0193. Available at: doi:10.1002/hbm.20750

[31] LACHAUX, Jean-Philippe, Nikolai AXMACHER, Florian MORMANN, Eric HALGREN and Nathan E. CRONE. *High-frequency neural activity and human cognition: Past, present and possible future of intracranial EEG research* [online]. 2012. ISBN 1873-5118 (Electronic)r0301-0082 (Linking). Available at: doi:10.1016/j.pneurobio.2012.06.008

[32] TALLON-BAUDRY, Catherine and Olivier BERTRAND. *Oscillatory gamma activity in humans and its role in object representation* [online]. 1999. ISBN 1879-307X (Electronic)n1364-6613 (Linking). Available at: doi:10.1016/S1364-6613(99)01299-1

[33] RAY, Supratim, Nathan E CRONE, Ernst NIEBUR, Piotr J FRANASZCZUK and Steven S HSIAO. Neural correlates of high-gamma oscillations (60-200 Hz) in macaque local field potentials and their potential implications in electrocorticography. *The Journal of neuroscience : the official journal of the Society for Neuroscience* [online]. 2008, vol. 28, pp. 11526–11536. ISSN 0270-6474. Available at: doi:10.1523/JNEUROSCI.2848-08.2008

[34] WILSON, M A and B L MCNAUGHTON. Reactivation of hippocampal ensemble memories during sleep. *Science (New York, N.Y.)* [online]. 1994, vol. 265, pp. 676–679. ISSN 0036-8075. Available at: doi:10.1126/science.8036517

[35] JADHAV, S. P., C. KEMERE, P. W. GERMAN and L. M. FRANK. *Awake Hippocampal Sharp-Wave Ripples Support Spatial Memory* [online]. 2012. ISBN 0036807510959203. Available at: doi:10.1126/science.1217230

[36] SULLIVAN, David, Jozsef CSICSVARI, Kenji MIZUSEKI, Sean MONTGOMERY, Kamran DIBA and György BUZSÁKI. Relationships between hippocampal sharp waves, ripples, and fast gamma oscillation: influence of dentate and entorhinal cortical activity. *The Journal of neuroscience : the official journal of the Society for Neuroscience* [online]. 2011, vol. 31, pp. 8605–8616. ISSN 0270-6474. Available at: doi:10.1523/JNEUROSCI.0294-11.2011

[37] AXMACHER, Nikolai, Christian E ELGER and Juergen FELL. Ripples in the medial temporal lobe are relevant for human memory consolidation. *Brain : a journal of neurology* [online]. 2008, vol. 131, pp. 1806–1817. ISSN 1460-2156. Available at: doi:10.1093/brain/awn103

[38] BRAGIN, Anatol, J ENGEL, C L WILSON, I FRIED and György BUZSÁKI. High-frequency oscillations in human brain. *Hippocampus* [online]. 1999, vol. 9, no. 2, pp. 137–42. ISSN 1050-9631. Available at: doi:10.1002/(SICI)1098-1063(1999)9:2<137::AID-HIPO5>3.0.CO;2-0

[39] ENGEL, Jerome, Anatol BRAGIN, Richard J STABA and Istvan MODY. High-frequency oscillations: what is normal and what is not? *Epilepsia* [online]. 2009, vol. 50, no. 4, pp. 598–604 [accessed. 2014-01-22]. ISSN 1528-1167. Available at: doi:10.1111/j.1528-1167.2008.01917.x

[40] MATSUMOTO, Joseph Y, Matt STEAD, Michal T. KUCEWICZ, Andrew J MATSUMOTO, Pierce a PETERS, Benjamin H BRINKMANN, Jane C DANSTROM, Stephan J GOERSS, W Richard MARSH, Fred B MEYER and Gregory a WORRELL. Network oscillations modulate interictal epileptiform spike rate during human memory. *Brain : a journal of neurology* [online]. 2013, vol. 136, no. Pt 8, pp. 2444–56 [accessed. 2013-11-08]. ISSN 1460-2156. Available at: doi:10.1093/brain/awt159

[41] STABA, Richard J, Charles L WILSON, Anatol BRAGIN, Itzhak FRIED and Jerome ENGEL. Quantitative Analysis of High-Frequency Oscillations (80 − 500 Hz) Recorded in Human Epileptic Hippocampus and Entorhinal Cortex. *Journal of neurophysiology*. 2002, vol. 88, pp. 1743–1752.

[42] WORRELL, Gregory A, Andrew B GARDNER, S Matt STEAD, Sanqing HU, Steve GOERSS, Gregory J CASCINO, Fredric B MEYER, Richard MARSH and Brian LITT. High-frequency oscillations in human temporal lobe: simultaneous microwire and clinical macroelectrode recordings. *Brain* [online]. 2008, vol. 131, no. Pt 4, pp. 928–937. Available at: doi:10.1093/brain/awn006.High-frequency

[43] JACOBS, Julia, Pierre LEVAN, Claude-Edouard CHÂTILLON, André OLIVIER, François DUBEAU and Jean GOTMAN. High frequency oscillations in intracranial EEGs mark epileptogenicity rather than lesion type. *Brain : a journal of neurology* [online]. 2009, vol. 132, no. Pt 4, pp. 1022–37 [accessed. 2013-11-25]. ISSN 1460-2156. Available at: doi:10.1093/brain/awn351

[44] BAGSHAW, Andrew P, Julia JACOBS, Pierre LEVAN, François DUBEAU and Jean GOTMAN. Effect of sleep stage on interictal high-frequency oscillations recorded from depth macroelectrodes in patients with focal epilepsy. *Epilepsia* [online]. 2009, vol. 50, no. 4, pp. 617–28 [accessed. 2014-01-22]. ISSN 1528-1167. Available at: doi:10.1111/j.1528-1167.2008.01784.x

[45] BRÁZDIL, Milan, Josef HALÁMEK, Pavel JURÁK, Pavel DANIEL, Robert KUBA, Jan CHRASTINA, Zdenek NOVÁK and Ivan REKTOR. Interictal high-frequency oscillations indicate seizure onset zone in patients with focal cortical dysplasia. *Epilepsy research* [online]. 2010, vol. 90, no. 1-2, pp. 28–32 [accessed. 2014-01-22]. ISSN 1872-6844. Available at: doi:10.1016/j.eplepsyres.2010.03.003

[46] CRÉPON, Benoît, Vincent NAVARRO, Dominique HASBOUN, Stéphane CLEMENCEAU, Jacques MARTINERIE, Michel BAULAC, Claude ADAM and Michel LE VAN QUYEN. Mapping interictal oscillations greater than 200 Hz recorded with intracranial macroelectrodes in human epilepsy. *Brain : a journal of neurology* [online]. 2010, vol. 133, no. Pt 1, pp. 33–45 [accessed. 2014-01-22]. ISSN 1460-2156. Available at: doi:10.1093/brain/awp277

[47] JACOBS, Julia, Maeike ZIJLMANS, Rina ZELMANN, Claude-Edouard CHATILLON, Jeffrey HALL, André OLIVIER, François DUBEAU and Jean GOTMAN. High-frequency electroencephalographic oscillations correlate with outcome of epilepsy surgery. *Annals of neurology* [online]. 2010, vol. 67, no. 2, pp. 209–20 [accessed. 2014-01-11]. ISSN 1531-8249. Available at: doi:10.1002/ana.21847

[48] WU, J Y, R SANKAR, J T LERNER, Joseph Y MATSUMOTO, H V VINTERS and G W MATHERN. Removing interictal fast ripples on electrocorticography linked with seizure freedom in children. *Neurology* [online]. 2010, vol. 75, no. 19, pp. 1686–94 [accessed. 2014-01-29]. ISSN 1526-632X. Available at: doi:10.1212/WNL.0b013e3181fc27d0

[49] GROSS, D W and J GOTMAN. Correlation of high-frequency oscillations with the sleep-wake cycle and cognitive activity in humans. *Neuroscience* [online]. 1999, vol. 94, no. 4, pp. 1005–18. ISSN 0306-4522. Available at: http://www.ncbi.nlm.nih.gov/pubmed/10625043

[50] WORRELL, Gregory A, Landi PARISH, Stephen D CRANSTOUN, Rachel JONAS, Gordon BALTUCH and Brian LITT. High-frequency oscillations and seizure generation in neocortical epilepsy. *Brain : a journal of neurology* [online]. 2004, vol. 127, no. Pt 7, pp. 1496–506 [accessed. 2014-01-22]. ISSN 0006-8950. Available at: doi:10.1093/brain/awh149

[51] GARDNER, Andrew B, Gregory A WORRELL, Eric MARSH, Dennis DLUGOS and Brian LITT. Human and automated detection of high-frequency oscillations in clinical intracranial EEG recordings. *Clinical Neurophysiology* [online]. 2007, vol. 118, pp. 1134–1143.

[52] BLANCO, Justin A, S Matt STEAD, Abba KRIEGER, Jonathan VIVENTI, W Richard MARSH, Kendall H LEE, Gregory A WORRELL and Brian LITT. Unsupervised classification of high-frequency oscillations in human neocortical epilepsy and control patients. *Journal of neurophysiology* [online]. 2010, vol. 104, no. 5, pp. 2900–2912 [accessed. 2013-10-24]. ISSN 1522-1598. Available at: doi:10.1152/jn.01082.2009

[53] PEARCE, Allison, Drausin WULSIN, Justin A BLANCO, Abba KRIEGER, Brian LITT and William C STACEY. Temporal changes of neocortical high-frequency oscillations in epilepsy. *Journal of neurophysiology* [online]. 2013, vol. 110, no. 5, pp. 1167–79 [accessed. 2013-10-26]. ISSN 1522-1598. Available at: doi:10.1152/jn.01009.2012

[54] ZELMANN, Rina, F MARI, Julia JACOBS, Maeike ZIJLMANS, Rahul CHANDER and J GOTMAN. Automatic detector of High Frequency Oscillations for human recordings with macroelectrodes. In: *32nd Annual International Conference of the IEEE EMBS*. 2010, p. 2329–2333. ISBN 9781424441242.

[55] NELSON, Ryan, Stephen M MYERS, Jennifer D SIMONOTTO, Michael D FURMAN, Mark SPANO, Wendy M NORMAN, Zhao LIU, Thomas B DEMARSE, Paul R CARNEY and William L DITTO. Detection of high frequency oscillations with Teager energy in an animal model of limbic epilepsy. In: *Conference proceedings : ... Annual International Conference of the IEEE Engineering in Medicine and Biology Society. IEEE Engineering in Medicine and Biology Society. Conference*. 2006, p. 2578–2580. ISBN 1424400333.

[56] MARAGOS, Petros, James F. KAISER and Thomas F. QUATIERI. On Amplitude and Frequency Demodulation Using Energy Operators. *Transactions on signal processing*. 1993, vol. 41, no. 4, pp. 1532–1550.

[57] DÜMPELMANN, Matthias, Julia JACOBS, Karolin KERBER and Andreas SCHULZE-BONHAGE. Automatic 80-250Hz 'ripple' high frequency oscillation detection in invasive subdural grid and strip recordings in epilepsy by a radial basis function neural network. *Clinical neurophysiology : official journal of the International Federation of Clinical Neurophysiology* [online]. 2012, vol. 123, no. 9, pp. 1721–31 [accessed. 2016-01-16]. ISSN 1872-8952. Available at: doi:10.1016/j.clinph.2012.02.072

[58] LÓPEZ-CUEVAS, Armando, Bernardino CASTILLO-TOLEDO, Laura MEDINA-CEJA, Consuelo VENTURA-MEJÍA and Kenia PARDO-PEÑA. An algorithm for on-line detection of high frequency oscillations related to epilepsy. *Computer methods and programs in biomedicine* [online]. 2013, vol. 110, no. 3, pp. 354–60 [accessed. 2013-10-26]. ISSN 1872-7565. Available at: doi:10.1016/j.cmpb.2013.01.014

[59] PINCUS, Steven M. Approximate entropy as a measure of system complexity. In: *Proceedings of National Academy of Sciences 1991*.

[60] LIANG, Sheng-Fu, Kuo-Tien LEE, Yu-Hsiang PAN and Yung-Hung WANG. Fast computation of sample entropy and approximate entropy in biomedicine. *Computer Methods and Programs in Biomedicine* [online]. 2011, vol. 104, no. 3, pp. 382–396 [accessed. 2013-10-26]. ISSN 1872-7565. Available at: doi:10.1016/j.cmpb.2010.12.003

[61] CHAIBI, Sahbi, Zied SAKKA, Tarek LAJNEF, Mounir SAMET and Abdennaceur KACHOURI. Automated detection and classification of high frequency oscillations (HFOs) in human intracereberal EEG. *Biomedical Signal Processing and Control* [online]. 2013, vol. 8, no. 6, pp. 927–934 [accessed. 2014-02-14]. ISSN 17468094. Available at: doi:10.1016/j.bspc.2013.08.009

[62] BIROT, Gwénaël, Amar KACHENOURA, Laurent ALBERA, Christian BÉNAR and Fabrice WENDLING. Automatic detection of fast ripples. *Journal of neuroscience methods* [online]. 2013, vol. 213, no. 2, pp. 236–49 [accessed. 2016-01-16]. ISSN 1872-678X. Available at: doi:10.1016/j.jneumeth.2012.12.013

[63] BURNOS, Sergey, Peter HILFIKER, Oguzkan SÜRÜCÜ, Felix SCHOLKMANN, Niklaus KRAYENBÜHL, Thomas GRUNWALD and Johannes SARNTHEIN. Human intracranial high frequency oscillations (HFOs) detected by automatic time-frequency analysis. *PloS one* [online]. 2014, vol. 9, no. 4, p. e94381 [accessed. 2016-01-16]. ISSN 1932-6203. Available at: doi:10.1371/journal.pone.0094381

[64] ZELMANN, Rina, F MARI, Julia JACOBS, Maeike ZIJLMANS, François DUBEAU and Jean GOTMAN. A comparison between detectors of high frequency oscillations. *Clinical Neurophysiology* [online]. 2012, vol. 123, no. 1, pp. 106–116 [accessed. 2013-10-26]. ISSN 1872-8952. Available at: doi:10.1016/j.clinph.2011.06.006

[65] DÜMPELMANN, Matthias, Julia JACOBS, Karolin KERBER and Andreas SCHULZE-BONHAGE. Automatic 80-250Hz 'ripple' high frequency oscillation detection in invasive subdural grid and strip recordings in epilepsy by a radial basis function neural network. *Clinical neurophysiology : official journal of the International Federation of Clinical Neurophysiology* [online]. 2012, vol. 123, no. 9, pp. 1721–31. ISSN 1872-8952. Available at: doi:10.1016/j.clinph.2012.02.072

[66] TRAVNICEK, Vojtech. *Interactive spatial visualisation of eeg parameters from depth intracranial electrodes in CT/MRI images*. B.m., 2015. Brno University of Technology.

[67] CIMBALNIK, Jan, Michal T. KUCEWICZ and Gregory a WORRELL. Interictal high-frequency oscillations in focal human epilepsy. *Current Opinion in Neurology* [online]. 2016, no. February, pp. 175–181. ISSN 1350-7540. Available at: doi:10.1097/WCO.0000000000000302

[68] KUCEWICZ, Michal T., Jan CIMBALNIK, Joseph Y MATSUMOTO, Benjamin H BRINKMANN, Mark R BOWER, Vincent VASOLI, Vlastimil SULC, Fred MEYER, W R MARSH, S M STEAD and Gregory a WORRELL. High frequency oscillations are associated with cognitive processing in human recognition memory. *Brain : a journal of neurology* [online]. 2014, pp. 1–14 [accessed. 2014-06-15]. ISSN 1460-2156. Available at: doi:10.1093/brain/awu149

LIST OF SYMBOLS, VARIABLES AND ABBREVIATIONS

EEG	Electroencephalograph
AED	Anti-epileptic drug
iEEG	Intracranial EEG
sEEG	Stereo EEG
SOZ	Seizure onset zone
MRI	Magnetic resonance imaging
CT	Computed tomography
fMRI	Functional magnetic resonance imaging
PET	Positron emission tomography
SPECT	Single photon emission tomography
MEG	Magnetoencephalography
HFO	High-frequency oscillation
ROC	Receiver operating curve
AUC	Area under the curve
FNUSA	St. Anne's University Hospital in Brno
ICU	Intensive care unit
LFP	Local field potential
FFP	Far field potential

LIST OF SUPPLEMENTS

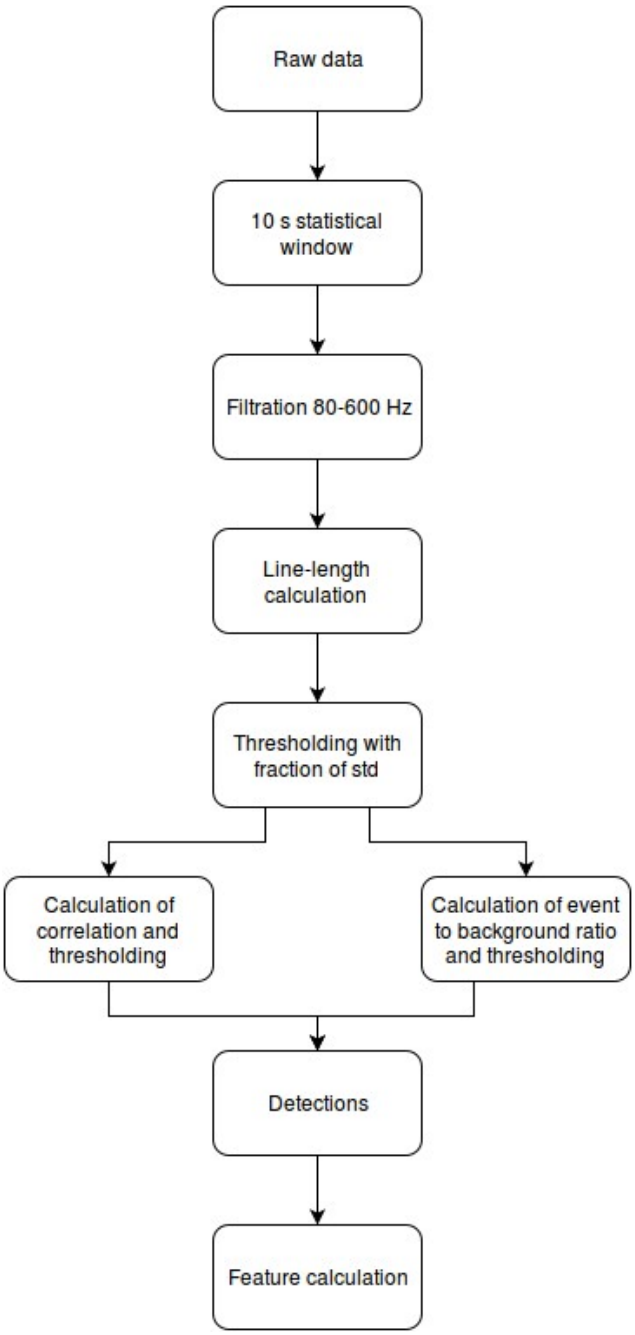

Supplement 1: ***Block diagram of line-length algorithm.***

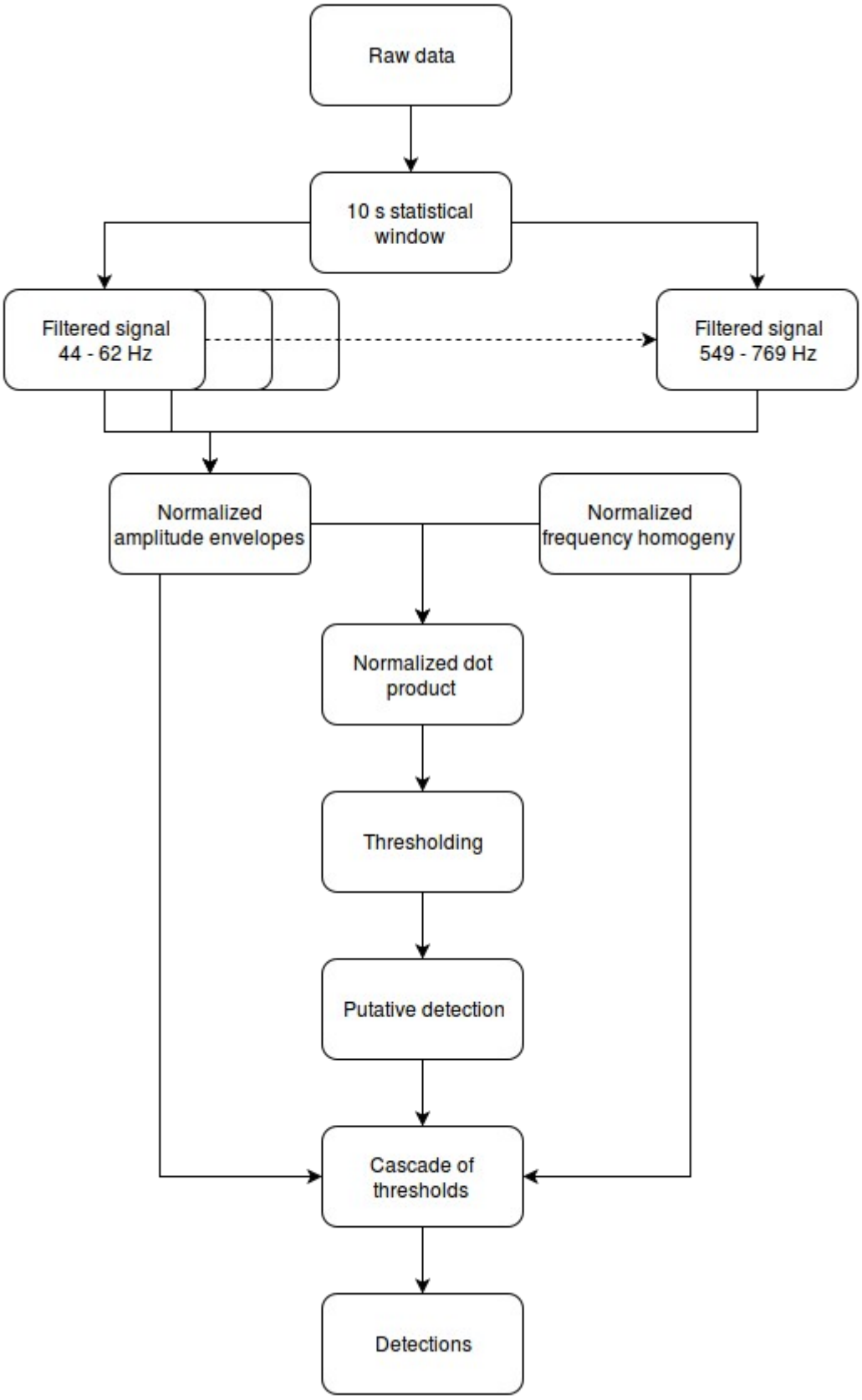

Supplement 2: ***Block diagram of frequency homogeny algorithm.***

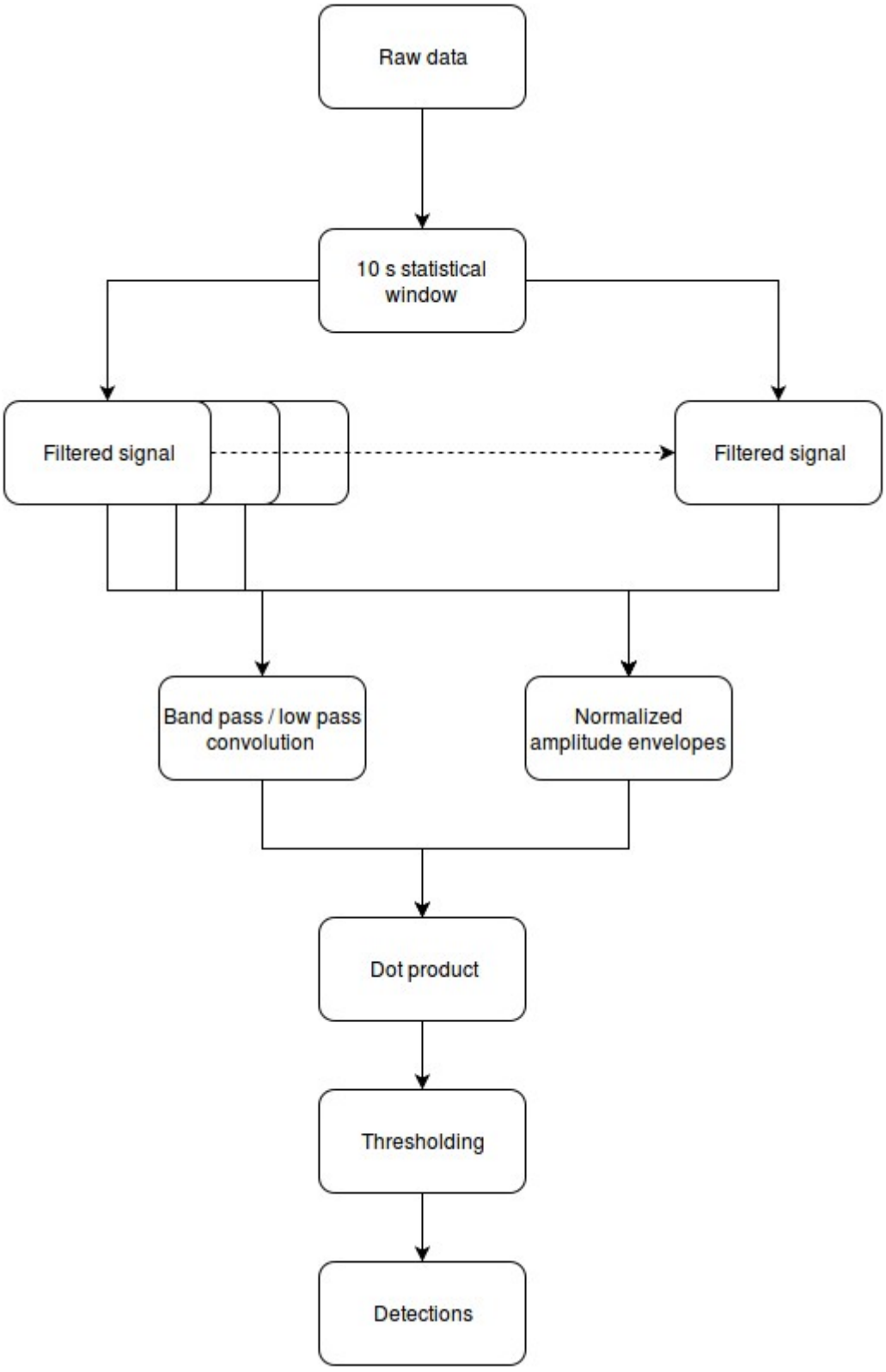

Supplement 3: ***Block diagram of Hilbert detection algorithm.***

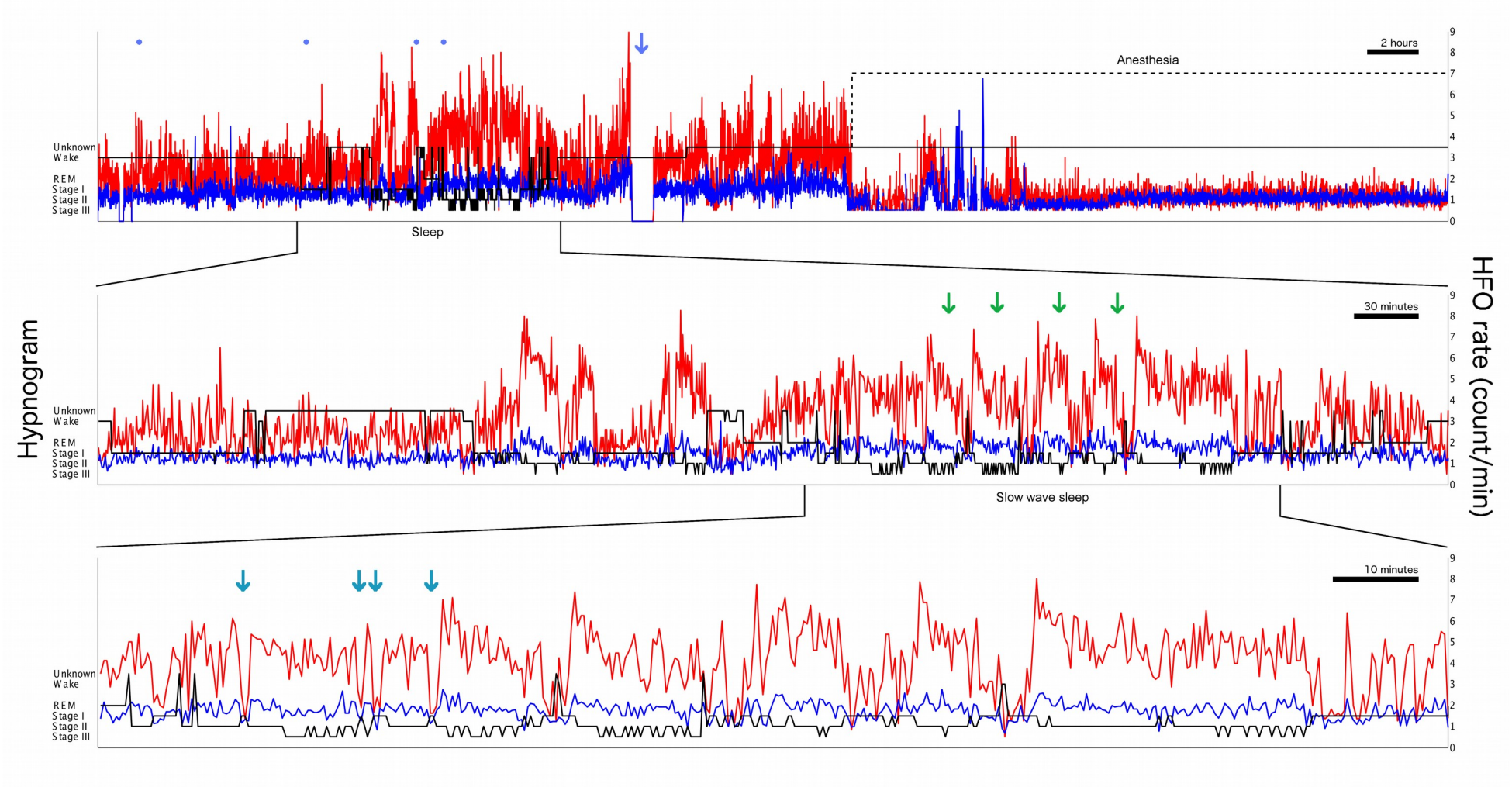

Supplement 4: ***HFO rates during sleep.***

Top – whole recording, middle – sleep part of the recording, bottom – slow wave part of the recording. Red – HFO rate in SOZ channels, blue – HFO rate in nonSOZ channels, black – hypnogram. Note the oscillatory peaks in HFO rates that correlate with slow wave sleep (green arrows) and even with slight changes in hypnogram (teal arrows).